Magnetogenesis from axion-SU(2) inflation

Journal of Cosmology and Astroparticle Physics
An IOP and SISSA journal

Received: *September 10, 2024*
Accepted: *November 18, 2024*
Published: *December 20, 2024*

Magnetogenesis from axion-SU(2) inflation

Axel Brandenburg[a,b,c,d], **Oksana Iarygina**[a,b], **Evangelos I. Sfakianakis**[e] and **Ramkishor Sharma**[f,a]

[a] *Nordita, KTH Royal Institute of Technology and Stockholm University, Hannes Alfvéns väg 12, 106 91 Stockholm, Sweden*
[b] *The Oskar Klein Centre, Department of Astronomy, Stockholm University, 106 91 Stockholm, Sweden*
[c] *McWilliams Center for Cosmology & Department of Physics, Carnegie Mellon University, Pittsburgh, PA 15213, U.S.A.*
[d] *School of Natural Sciences and Medicine, Ilia State University, 3-5 Cholokashvili Avenue, 0194 Tbilisi, Georgia*
[e] *Department of Physics, Case Western Reserve University, 10900 Euclid Avenue, Cleveland, OH 44106, U.S.A.*
[f] *CEICO, FZU-Institute of Physics of the Czech Academy of Sciences, Na Slovance 1999/2, 182 00 Prague 8, Czech Republic*

E-mail: brandenb@nordita.org, oksana.iarygina@su.se, esfakianakis@ifae.es, sharma@fzu.cz

Abstract: We describe a novel proposal for inflationary magnetogenesis by identifying the non-Abelian sector of Spectator Chromo Natural Inflation (SCNI) with the $SU(2)_L$ sector of the Standard Model. This mechanism relies on the recently discovered attractor of SCNI in the strong backreaction regime, where the gauge fields do not decay on super-horizon scales and their backreaction leads to a stable new trajectory for the rolling axion field. The large super-horizon gauge fields are partly transformed after the electroweak phase transition into electromagnetic fields. The strength and correlation length of the resulting helical magnetic fields depend on the inflationary Hubble scale and the details of the SCNI sector. For suitable parameter choices we show that the strength of the resulting magnetic fields having correlation lengths around 1 Mpc are consistent with the required intergalactic magnetic fields for explaining the spectra of high energy γ rays from distant blazars.

Keywords: physics of the early universe, primordial magnetic fields, inflation

ArXiv ePrint: 2408.17413

https://doi.org/10.1088/1475-7516/2024/12/057

JCAP12(2024)057

Contents

1 Introduction

The presence of magnetic fields is ubiquitous in our universe [1–7]. Particularly intriguing is the evidence for extragalactic magnetic fields arising from the observations of distant blazars. The non-detection of the secondary GeV photons in blazar observations points towards the existence of extragalactic magnetic fields (EGMFs) between us (the observer) and the distant blazars [8–15]. The strength of the magnetic field that is necessary to explain the blazar observations depends on its correlation length, L. For $L \geq 0.1\,\mathrm{Mpc}$, the typical magnetic field $B_{0.1\,\mathrm{Mpc}}$, needs to be larger than $10^{-15}\,\mathrm{G}$, or $10^{-17}\,\mathrm{G}$, depending on the assumptions made about the dynamics of the electromagnetic cascade and secondary GeV γ-ray emission [12]. For $L < 0.1\,\mathrm{Mpc}$, the typical magnetic field $B = B_{0.1\,\mathrm{Mpc}}\sqrt{0.1\,\mathrm{Mpc}/\mathrm{L}}$ can be even larger.

While there is no conclusive answer to the question of the origin of EGMFs, many proposals have been put forth (see, e.g., refs. [16–20]). For simplicity, we can categorize these proposals into those involving inflation and reheating [21–39], and those focusing on early universe phase transitions (including QCD and electroweak) [40–48]. In this work we focus on inflationary magnetogenesis, which encompasses a plethora of models and continues to be a rich area of research. Since Maxwell's action is conformally invariant, there can be no significant magnetic field production during inflation, unless some way of breaking

JCAP12(2024)057

conformal invariance is introduced. A simple way is to couple a U(1) gauge field, e.g., the electromagnetic (EM) or hypercharge gauge boson of the Standard Model, to the rolling inflaton or some other dynamical (pseudo)scalar field during inflation. Usual couplings include the terms $I(\phi)F_{\mu\nu}F^{\mu\nu}$ or $I(\phi)F_{\mu\nu}\tilde{F}^{\mu\nu}$, where $I(\phi)$ is some function of the scalar field ϕ. The former is usually referred to as the Ratra model [22] and we will not discuss it further (see, e.g., refs. [26, 49] for non-Gaussianities and the strong coupling problem in the Ratra model).

We focus on the axial coupling term $I(\phi)F_{\mu\nu}\tilde{F}^{\mu\nu}$, which results in the production of helical fields [50]. The importance of helical magnetic fields in the context of inflationary magnetogenesis has been mainly based on the inverse cascade effect [51, 52]. During the inverse cascade process, power is transferred from short- to long-wavelength modes, thereby slowing down the decay, and at the same time increasing the correlation length [53]. The coupling of axions to gauge fields during inflation has been extensively studied. The phenomenology includes the amplification of parity violating gauge fields during slow-roll inflation [23, 54, 55] and their influence on the inflationary dynamics [56–59], as well as the generation of metric fluctuations by a rolling auxiliary pseudo-scalar field during inflation [60–64]. The produced gauge fields can backreact on the axion [65–75], possibly leading to significant non-Gaussianity [76, 77]. The strength of the axion-gauge coupling must be constrained to keep non-Gaussianity of the density fluctuations, chiral gravitational waves, and the production of primordial black holes within observational limits [58, 59, 76, 78, 79]. The authors of ref. [33] showed that a simple model of axion inflation coupled to the hypercharge field of the SM leads to very fast preheating; almost the entirety of the energy density of the inflaton is transferred to gauge fields within one e-fold after the end of inflation. The resulting gauge field spectrum has a significant degree of helicity and its amplitude is large enough to lead to present-day magnetic fields that are compatible with blazar observations. The parameters chosen allowed for both instantaneous preheating and efficient magnetogenesis, while at the same time not violating bounds from non-Gaussianity and primordial black hole production.

A seemingly straightforward extension of natural inflation [80] coupled to an Abelian gauge field, is the coupling of the axion-inflaton to a non-Abelian field instead. The non-trivial vacuum structure of the SU(2) sector [81, 82] and its interplay with the axion field leads to a new inflationary attractor, in which the gauge field produces an extra source of friction, allowing for slow-roll inflation even in steep potentials [83–87]. This model goes under the name Chromo-Natural Inflation (CNI). Similarly to the Abelian field case, the tensor modes of the SU(2) sector experience an instability, which causes one polarization to become exponentially amplified. The amplified SU(2) tensors seed gravitational waves, which are also chiral. The original version of Chromo-Natural inflation (one involving a cosine potential) has been shown to be incompatible with CMB observations [83], producing either too large tensor-to-scalar ratio r or too small scalar spectral index n_s. By invoking spontaneous breaking of the SU(2) symmetry, the resulting model of Higgsed Chromo-Natural Inflation [88] produces primordial observables which are observationally allowed for certain parts of parameter space, while evading the Lyth bound [89] and generating observable gravitational waves at a lower inflationary scale. Furthermore, the resulting tensor spectral tilt n_T generically violates the consistency relation $r = -8n_T$, where r is the tensor to scalar ratio and n_T is the spectral index of the tensor modes. Alternative ways to bring CNI in

JCAP12(2024)057

agreement with CMB data include modifying the potential of the axion field [86, 90], delaying the CNI phase such that gravitational waves production happens at higher frequencies than CMB [91–93] and introducing non-minimal coupling to gravity [94, 95]. Finally, by integrating out the axion field, a non-linear term is introduced involving the gauge field strength, which leads to similar behavior and phenomenology [96–100].

An interesting extension of CNI was proposed in ref. [101], where the axion-SU(2) action was treated as a spectator sector. This allows the model to generate the tensor modes through the instability of the Chromo-Natural sector, while the scalar modes are produced by a dominant inflaton sector. This decoupling of the inflationary energy scale from the gravitational wave (GW) amplitude allows for very low scale inflation with observable GWs [102]. This model has been dubbed "spectator chromo-natural inflation" (SCNI) and has been shown to produce distinct GW spectra, depending on the shape of the axion potential [103].

We recently explored the effects of backreaction on the SCNI model [104], where we reported the emergence of a novel attractor, supported by the backreaction of super-horizon gauge field modes on the rolling axion. This novel backreaction-supported attractor was found numerically and further described using analytical arguments. Our results were subsequently independently verified in ref. [105], where the possibility of primordial black hole formation was pointed out. It is worth mentioning that pushing any nonlinear model to the strong backreaction regime can raise perturbativity issues. Ref. [106] recently showed that perturbativity bounds on the parameter space are similar to those arising from the onset of the strong backreaction regime. That being said, computing perturbativity bounds inside the strong backreaction regime requires using the full numerical solution of the equations of motion. So as not to deviate from the main point of the current paper, that of inflationary magnetogenesis, we leave the full analysis of perturbativity constraints for future work.

In the current work, we consider the model of spectator chromo-natural inflation, where we identify the SU(2) field as the weak sector of the Standard Model.[1] This can be thought of as the natural counterpart to natural inflation magnetogenesis, where the axion is coupled to the U(1) hypercharge sector. Even if the two models are similar in spirit, their analysis differs significantly due to the structure of the SCNI attractor and the richer structure of the fluctuations. The basic premise is the tachyonic generation of tensor modes of the SU(2) sector, equivalently weak bosons of the SM, during inflation. After the EW phase transition, the weak and hypercharge sectors mix and a component of the weak bosons is "transformed" into EM fields, which will also be helical to a large degree. After the generation of these EM fields, the electric part will be damped by the primordial plasma, while the magnetic part may undergo inverse cascading, thereby leading to the current length scales and field strengths of magnetic fields across the universe today [52, 108]. Furthermore, since we are interested in the evolution of the tensor modes from their generation during inflation until the electroweak phase transition (EWPT), we revisited SCNI by focusing on the end of inflation, which has been largely neglected in the literature so far. We thus point out the (rather generic) possibility of a second phase of inflation, where the chromo-natural sector

[1] A proposal to realize Chromo-Natural inflation using the Higgs as the inflaton [107] may lead to similar phenomenology, but is beyond the scope of this work.

JCAP12(2024)057

dominates. In order to avoid that, one must either add extra couplings to drain the energy from the chromo-natural sector or adjust (tune) the initial value of the axion field, such that the spectator axion reaches its minimum before or at most shortly after the end of inflation.

An interesting point regarding inflationary magnetogenesis arises from the baryon isocurvature perturbations, which were computed in detail in ref. [109]. Due to the unknown details of the EWPT, the computation of the baryon number (and correspondingly the spatial variations of the baryon number) will necessarily include uncertainties (see, e.g., ref. [110]). While ref. [109] provides serious challenges on inflationary magnetogenesis, we leave a detailed evaluation of the baryon isocurvature perturbations in our model (and possible effects of BSM-generated alterations to the nature of the EWPT) for future work.

This work is organized as follows. In section 2, we review the spectator chromo-natural inflation model, its background dynamics and perturbations. Further we demonstrate that, when the SU(2) sector of the model is associated with the Standard Model weak bosons, the system inevitably enters the strong backreaction regime and converges to the recently discovered backreaction-supported attractor. In section 3 we investigate the dynamics of the background quantities and perturbations at the end of inflation. We show that, when by the end of inflation the axion field does not reach the minimum of its potential, the system enters a second inflationary phase dominated by the axion-SU(2) sector. Further in section 4, we study the evolution of perturbations after inflation and discuss the magnetic field generation. We conclude in section 5.

2 Model and attractor behavior

In this section we introduce the model and background evolution of the system. We further discuss the backreaction constraints and indicate their immediate importance when the SU(2) sector of the model is associated with the Standard Model weak bosons. We provide a brief review of perturbations in axion-SU(2) inflation and their backreaction on the background evolution, along with the subsequent convergence of axion field and the gauge field vacuum expectation value (VEV) to the new dynamical attractor.

2.1 Background evolution

The action for spectator axion-SU(2) inflation is given by [101]

$$S = \int d^4x\sqrt{-g}\left(\frac{M_{\rm pl}^2}{2}R - \frac{1}{2}(\partial\phi)^2 - V(\phi) - \frac{1}{2}(\partial\chi)^2 - U(\chi) - \frac{1}{4}F^a_{\mu\nu}F^{a\,\mu\nu} + \frac{\lambda\chi}{4f}F^a_{\mu\nu}\tilde{F}^{a\,\mu\nu}\right), \tag{2.1}$$

where $g \equiv \det g_{\mu\nu}$, R is the space-time Ricci scalar, $\phi(t)$ is the inflaton field, $\chi(t)$ is the axion, λ is the coupling constant between the gauge and axion sectors, f is the axion decay constant, and $M_{\rm pl}$ is the reduced Planck mass. The field strength of the SU(2) gauge field is

$$F^a_{\mu\nu} = \partial_\mu A^a_\nu - \partial_\nu A^a_\mu - g\epsilon^{abc}A^b_\mu A^c_\nu, \tag{2.2}$$

with g being the gauge field coupling. $\tilde{F}^{a\,\mu\nu} = \epsilon^{\mu\nu\rho\sigma}F^a_{\rho\sigma}/\left(2\sqrt{-\det g_{\mu\nu}}\right)$ is a dual of the gauge field strength and $\epsilon^{\mu\nu\alpha\beta}$ is the antisymmetric tensor normalized as $\epsilon^{0123} = 1$.

JCAP12(2024)057

We use an axion potential of the form

$$U(\chi) = \mu^4 \left(1 + \cos\frac{\chi}{f}\right), \tag{2.3}$$

where μ is a constant that sets the energy scale of the axion potential. Without loss of generality, we restrict the axion field to be in the interval $\chi \in [0, \pi f]$. In the SCNI model, the inflationary sector is responsible for the generation of the observed density fluctuations. Instead of modelling the inflationary dynamics as a quasi de-Sitter expansion, we choose to impose concrete inflationary potentials, $V(\phi)$, which are specified in section 3.

We work with the Friedmann-Lemaître-Robertson-Walker (FLRW) metric

$$ds^2 = -dt^2 + a(t)^2 \delta_{ij} dx^i dx^j, \tag{2.4}$$

where i, j represent the spatial indices and $a(t)$ is the scale factor. For SCNI the isotropic gauge field configuration at the background level is an attractor [111] and is given by [81, 82]

$$A^a_0 = 0, \qquad A^a_i = \delta^a_i a(t) Q(t). \tag{2.5}$$

For the action (2.1) and the isotropic gauge field configuration (2.5) the background system of equations for the inflaton field, the axion, and the gauge field vacuum expectation value is given by

$$M_{\rm pl}^2 \dot{H} = -\frac{1}{2}\dot{\phi}^2 - \frac{1}{2}\dot{\chi}^2 - \left((\dot{Q}+HQ)^2 + g^2Q^4\right), \tag{2.6}$$

$$3M_{\rm pl}^2 H^2 = \frac{\dot{\phi}^2}{2} + V(\phi) + \frac{\dot{\chi}^2}{2} + U(\chi) + \frac{3}{2}\left(\dot{Q}+HQ\right)^2 + \frac{3}{2}g^2Q^4, \tag{2.7}$$

$$\ddot{Q} + 3H\dot{Q} + \left(\dot{H} + 2H^2\right)Q + 2g^2Q^3 = \frac{g\lambda}{f}\dot{\chi}Q^2, \tag{2.8}$$

$$\ddot{\chi} + 3H\dot{\chi} + U_\chi(\chi) = -\frac{3g\lambda}{f}Q^2\left(\dot{Q}+HQ\right), \tag{2.9}$$

$$\ddot{\phi} + 3H\dot{\phi} + V_\phi(\phi) = 0, \tag{2.10}$$

where an overdot denotes a derivative with respect to cosmic time t, $H = \dot{a}/a$ is the Hubble parameter, $V_\phi(\phi) = \partial V(\phi)/\partial\phi$ and $U_\chi(\chi) = \partial U(\chi)/\partial\chi$.

A viable inflationary model requires $f, \mu \ll M_{\rm pl}$ with the energy scale of inflation being well below the cut-off of the effective theory $f/\lambda \gg H$. Furthermore, the existence of the chromo-natural attractor solution [85] restricts the parameter space to $\Lambda \equiv \lambda Q/f \gg \min(\sqrt{2}, \sqrt{3}H/gQ)$. When the above conditions are satisfied, the chromo-natural inflation model in the slow-roll approximation approaches the attractor [83, 85]

$$\frac{\lambda}{f}\dot{\chi} = 2gQ + \frac{2H^2}{gQ}, \qquad \dot{Q} = -HQ + \frac{f}{3g\lambda}\frac{U_\chi}{Q^2}. \tag{2.11}$$

Moreover, to ensure that scalar perturbations are controlled by the inflaton field, we impose the spectator condition that the energy densities of the axion field and gauge sector are subdominant to that of the inflaton, i.e.,

$$\rho_\phi \gg \rho_{Q_E},\, \rho_{Q_B},\, \rho_\chi, \tag{2.12}$$

JCAP12(2024)057

where the corresponding energy densities are given by

$$\rho_\phi = \frac{1}{2}\dot{\phi}^2 + V(\phi), \quad \rho_{Q_E} = \frac{3}{2}(\dot{Q} + HQ)^2, \quad \rho_{Q_B} = \frac{3}{2}g^2Q^4, \quad \rho_\chi = \frac{1}{2}\dot{\chi}^2 + U(\chi). \tag{2.13}$$

The stability of scalar perturbations of the gauge sector requires $gQ/H > \sqrt{2}$. We impose these criteria to be satisfied for the part of inflation that corresponds to CMB scales.[2]

Finally, we assume that the inflaton field ϕ, along with the spectator sector comprised of the axion χ and the VEV of the gauge field Q, are slowly rolling during inflation, i.e., their slow-roll parameters are smaller than unity. The first slow-roll parameter ϵ_H is defined as

$$\epsilon_H = -\frac{\dot{H}}{H^2} = \epsilon_\phi + \epsilon_{Q_E} + \epsilon_{Q_B} + \epsilon_\chi, \tag{2.14}$$

with the contributions

$$\epsilon_\phi = \frac{\dot{\phi}^2}{2M_{\rm pl}^2H^2}, \quad \epsilon_{Q_E} = \frac{(\dot{Q} + HQ)^2}{M_{\rm pl}^2H^2}, \quad \epsilon_{Q_B} = \frac{g^2Q^4}{M_{\rm pl}^2H^2}, \quad \epsilon_\chi = \frac{\dot{\chi}^2}{2M_{\rm pl}^2H^2}. \tag{2.15}$$

2.2 Standard Model axion-SU(2) sector and backreaction

To study magnetogenesis from axion-SU(2) dynamics during inflation, we associate the Standard Model weak bosons with the SU(2) sector of the model.[3] Using the SM restricts the gauge coupling to be $g = \mathcal{O}(0.1)$, where we leave room for possible changes of the renormalization group flow to large energies due to unknown physics. As we will see, large gauge field couplings immediately push the system towards the strong backreaction regime.

It is convenient to introduce the parameters m_Q and ξ,

$$m_Q = \frac{gQ}{H}, \qquad \xi = \frac{\lambda}{2fH}\dot{\chi}, \tag{2.16}$$

which control the amplification of the gauge field fluctuations around horizon crossing and the subsequent sourcing of gravitational waves. When m_Q is approximately constant, the backreaction is small and can be neglected when [112]

$$g \ll \left(\frac{24\pi^2}{2.3 \cdot e^{3.9m_Q}} \frac{1}{1 + m_Q^{-2}}\right)^{1/2}. \tag{2.17}$$

Taking the smallest allowed value of $m_Q = \sqrt{2}$ to ensure the stability of scalar perturbations and evaluating the right-hand side of eq. (2.17) we get $g \ll 0.53$. It thus follows that gauge-field couplings $g \gtrsim \mathcal{O}(0.1)$ inevitably push the system into the strong backreaction regime.

[2] In this work, we focus on the study of tensor perturbations and leave a detailed analysis of scalar perturbations for future work.

[3] The axion coupled to the SM weak bosons has a mass of $m_\chi = \mu^2/f \gtrsim 10^{11}$ GeV (see table 1), which makes its effects in accelerator experiments unobservably small.

JCAP12(2024)057

2.3 Perturbations and the backreaction-supported attractor

The backreaction in chromo-natural inflation is caused by the tachyonic amplification of gauge field modes, which in turn backreact on the background dynamics and change it.

We choose the decomposition for field fluctuations following ref. [113]

$$\begin{aligned}
\phi &= \phi + \delta\phi, \\
\chi &= \chi + \delta\chi, \\
W_0^a &= a(Y_a + \partial_a Y), \\
W_i^a &= a\left[(Q+\delta Q)\,\delta_{ai} + \partial_i\left(M_a + \partial_a M\right) + \epsilon_{iac}\left(U_c + \partial_c U\right) + t_{ia}\right], \\
g_{00} &= -a^2\left(1-2\varphi\right), \\
g_{0i} &= a^2\left(B_i + \partial_i B\right), \\
g_{ij} &= a^2\left[(1+2\psi)\,\delta_{ij} + 2\partial_i\partial_j E + \partial_i E_j + \partial_j E_i + h_{ij}\right],
\end{aligned} \tag{2.18}$$

where $a = 1,2,3$ is the SU(2) index (not to be confused with the scale factor $a(t)$) and $i = 1,2,3$ is the index for spacial coordinates. Furthermore, t_{ia} and h_{ij} are the transverse and traceless tensor modes of gauge field and metric perturbations, respectively. Transverse vector modes are Y_a, M_a, U_c, B_i, E_i and scalar modes $\delta\phi$, $\delta\chi$, Y, δQ, M, φ, B.[4]

We focus on the tensor modes of the gauge field $t_{ia} \subset \delta W_i^a$ and the metric $h_{ij} \subset \delta g_{ij}$ and expand them into a helicity basis in Fourier space:

$$\begin{aligned}
t_{ij}(\mathbf{x},\tau) &= \int \frac{d^3k}{(2\pi)^{3/2}} e^{i\vec{k}\cdot\vec{x}} \sum_{\nu=\pm} \Pi^*_{ij,\nu}(\vec{k}) t_\nu(\tau,\vec{k}), \\
h_{ij}(\mathbf{x},\tau) &= \int \frac{d^3k}{(2\pi)^{3/2}} e^{i\vec{k}\cdot\vec{x}} \sum_{\nu=\pm} \Pi^*_{ij,\nu}(\vec{k}) h_\nu(\tau,\vec{k}),
\end{aligned} \tag{2.19}$$

where the polarization tensors satisfy [114]

$$\Pi^*_{ij,\pm}(\vec{k}) = \epsilon_{i,\pm}(\vec{k})\epsilon_{j,\pm}(\vec{k}), \tag{2.20}$$

and $\epsilon_{i,\pm}$ are helicity vectors with the properties

$$\begin{aligned}
\vec{k}\cdot\vec{\epsilon}_\pm(\vec{k}) = 0, \quad \vec{k}\times\vec{\epsilon}_\pm(\vec{k}) &= \mp ik\vec{\epsilon}_\pm(\vec{k}), \\
\vec{\epsilon}_\nu(\vec{k})\cdot\vec{\epsilon}^{\,*}_{\nu'}(\vec{k}) = \delta_{\nu\nu'}, \quad \vec{\epsilon}^{\,*}_\pm(\vec{k}) &= \vec{\epsilon}_\pm(-\vec{k}) = \vec{\epsilon}_\mp(\vec{k}).
\end{aligned} \tag{2.21}$$

We denote right- and left-handed modes $(\pm)$ as (R,L) and canonically normalize perturbations as

$$h_{R,L} = \frac{\sqrt{2}}{M_{\rm pl}a}\psi_{R,L}, \qquad t_{L,R} = \frac{1}{\sqrt{2}a}T_{R,L}. \tag{2.22}$$

[4]The scalar perturbation should not be confused with the magnetic field strength B.

JCAP12(2024)057

The equations of motion for perturbations up to $\mathcal{O}(\epsilon)$ are given by

$$\partial_t^2\psi_{R,L} + H\partial_t\psi_{R,L} + \left(\frac{k^2}{a^2} - 2H^2\right)\psi_{R,L}$$
$$= -2H\sqrt{\epsilon_{Q_E}}\partial_t T_{R,L} + 2H^2\sqrt{\epsilon_{Q_B}}\left(m_Q \mp \frac{k}{aH}\right)T_{R,L}, \tag{2.23}$$

$$\partial_t^2 T_{R,L} + H\partial_t T_{R,L} + \left(\frac{k^2}{a^2} + 2H^2\left(m_Q\xi \mp \frac{k}{aH}(m_Q+\xi)\right)\right)T_{R,L}$$
$$= 2H\sqrt{\epsilon_{Q_E}}\partial_t\psi_{R,L} + 2H^2\left(\sqrt{\epsilon_{Q_B}}\left(m_Q \mp \frac{k}{aH}\right) + \sqrt{\epsilon_{Q_E}}\right)\psi_{R,L}. \tag{2.24}$$

The exponential growth of the tensor modes backreacts on the background equations of motion [101, 102, 112, 115, 116]. To take into account the contribution from backreaction, the background equations of motion can be written as

$$\ddot{Q} + 3H\dot{Q} + \left(\dot{H} + 2H^2\right)Q + 2g^2Q^3 - \frac{g\lambda}{f}\dot{\chi}Q^2 + \mathcal{T}^Q_{\rm BR} = 0, \tag{2.25}$$

$$\ddot{\chi} + 3H\dot{\chi} + U_\chi(\chi) + \frac{3g\lambda}{f}Q^2\left(\dot{Q} + HQ\right) + \mathcal{T}^\chi_{\rm BR} = 0. \tag{2.26}$$

The backreaction terms $\mathcal{T}^Q_{\rm BR}$ and $\mathcal{T}^\chi_{\rm BR}$ contain the integrals over the mode functions and are defined as[5]

$$\mathcal{T}^Q_{\rm BR} = \frac{g}{3a^2}\int\frac{d^3k}{(2\pi)^3}\left(\xi H - \frac{k}{a}\right)|T_R|^2, \tag{2.27}$$

$$\mathcal{T}^\chi_{\rm BR} = -\frac{\lambda}{2a^3 f}\frac{d}{dt}\int\frac{d^3k}{(2\pi)^3}\left(a\,m_Q H - k\right)|T_R|^2. \tag{2.28}$$

The effect of homogeneous backreaction during axion-SU(2) dynamics was recently explored in ref. [104]. When the backreaction becomes strong, the solution converges to *the new dynamical attractor* with negative values of the gauge field VEV and decreased velocity of the axion field, given by [104]

$$\frac{\lambda}{f}\dot{\chi} \simeq -\frac{2H^2}{gQ}, \quad U_\chi = -\frac{3g\lambda}{f}HQ^3 + \frac{1}{\tilde{\alpha}}\left(4H^2Q + 2g^2Q^3\right), \tag{2.29}$$

where the parameter $\tilde{\alpha}$ is the ratio of the backreaction integrals

$$\tilde{\alpha} = \frac{\mathcal{T}^Q_{\rm BR}}{\mathcal{T}^\chi_{\rm BR}} \simeq \frac{2}{9}\frac{Hf}{\lambda g\,Q^2} \tag{2.30}$$

and Q is the VEV of the gauge field on the new attractor. The new solution (2.29) resembles the chromo-natural attractor solution (2.11), with an opposite sign for the VEV Q, smaller axion velocity, and a modified dependence of Q on U_χ.

Ref. [104] approximated inflation as having a constant Hubble parameter. Therefore, once the axion-SU(2) system converged to the new backreaction-supported attractor, it remained there indefinitely. In the current work we aim to trace the evolution of the gauge field

[5] For homogeneous backreaction the effect from spatial gradients of inflation and axion fields are neglected.

JCAP12(2024)057

Run	g	μ	χ_i/f	Q_i	m_{Q_i}	H_i	$n_{\rm min}$	$n_{\rm max}$	model
A1	0.1	5.35×10^{-4}	0.975π	1.26×10^{-4}	2.37	5.3×10^{-6}	1	11	Const H
A2	0.1	4.76×10^{-4}	0.96π	1.26×10^{-4}	2.37	5.3×10^{-6}	1	11	Const H
B	0.1	5.80×10^{-4}	0.982π	1.26×10^{-4}	2.36	5.3×10^{-6}	1	8	Quadratic
C1	0.1	5.35×10^{-4}	0.975π	1.26×10^{-4}	2.37	5.3×10^{-6}	1	11	α-attractor
C2	0.1	5.30×10^{-4}	0.974π	1.26×10^{-4}	2.37	5.3×10^{-6}	1	11	α-attractor
C3	0.1	5.25×10^{-4}	0.973π	1.26×10^{-4}	2.37	5.3×10^{-6}	1	11	α-attractor
D	0.65	1.60×10^{-4}	0.975π	1.35×10^{-5}	1.65	5.3×10^{-6}	-2	8	α-attractor
E	0.65	1.57×10^{-4}	0.973π	1.35×10^{-5}	1.65	5.3×10^{-6}	-2	8	α-attractor
F	0.1	3.79×10^{-4}	0.9π	1.26×10^{-4}	2.37	5.3×10^{-6}	1	8	α-attractor
G	0.1	1.24×10^{-3}	0.988π	3.04×10^{-4}	5.71	5.3×10^{-6}	1	8	α-attractor
H	0.1	5.25×10^{-4}	0.974π	1.25×10^{-4}	2.34	5.3×10^{-6}	1	11	α-attractor

Table 1. Parameters for the runs discussed in the paper. For all these runs $\lambda = 2000$. The value of $f = 0.09$ for runs with $g = 0.1$ and $f = 0.009$ for runs with $g = 0.65$. Here H_i represents the value of Hubble parameter at the start of the simulations. All dimensionful quantities are measured in units of $M_{\rm Pl}$.

perturbations from the end of inflation until the EWPT, in order to investigate the generation and evolution of magnetic fields. In the next section, we go beyond the results of ref. [104], by including the time dependence of the Hubble parameter in order to probe the dynamics of the gauge field perturbations and the background mode through the end of inflation.

3 Gauge-axion dynamics until the end of inflation

In this section we study the generation and evolution of tensor perturbations and model their evolution through the end of inflation. To depart from the approximation of a constant Hubble rate during inflation, we ran several simulations for different inflationary background models, specifically using quadratic and α-attractor potentials. The α-attractor potential is in agreement with CMB data and carries significant theoretical motivation [117, 118], whereas the quadratic potential can be thought of as an approximation of a more complicated potential, valid near the end of inflation, where the inflaton behaves as a massive scalar field. We provide the details of the parameters used for the different inflationary background models in section 3.1. The simulation parameters are summarized in table 1. The initial values of μ and χ/f were chosen to ensure that the initial Hubble parameter is the same and that the axion field χ approaches one of the minima of its potential at $f\pi/2$ before the end of inflation, except for run F. If χ does not reach the minimum of its potential before the end of inflation, the system will enter a second inflationary phase dominated by the axion-SU(2) sector, as we demonstrate later. This has been largely neglected in the spectator CNI literature so far and provides an important constraint on the viable parameter space of these models.

3.1 Background inflaton models

To probe the end of inflation, we use quadratic and α-attractor inflationary models for the background evolution. The details of the models are provided below. For the quadratic

JCAP12(2024)057

model, the potential of the scalar field has the usual form

$$V_{\rm quad} = \frac{1}{2}m^2\phi^2. \tag{3.1}$$

To achieve roughly sixty e-folds of inflation, we choose $\phi_i = 15.56\,M_{\rm Pl}$. The relevant mass scale is chosen as $m = 8.4\times10^{-7}\,M_{\rm Pl}$. These values lead to $H_i = 5.33\times10^{-6}\,M_{\rm Pl}$ at the initial time, which we take to coincide with the beginning of inflation.

In the case of α-attractors, the potential for the scalar field is given by,

$$V_{\alpha\text{-attr}}(\phi) = \alpha M\left((\tanh{(\beta\phi/2)})^2\right)^n, \tag{3.2}$$

where $\beta = \sqrt{2/3\alpha}$. In our simulations, we chose $\alpha = 1$, $M = 8.7\times10^{-11}\,M_{\rm Pl}$, $n = 3/2$, and the initial value of the scalar field, $\phi_{\rm in} = 6.7\,M_{\rm Pl}$, to achieve around sixty e-folds of inflation. In this case, $H_i = 5.32\times10^{-6}\,M_{\rm Pl}$ at the beginning of inflation.

3.2 Dynamics during inflation and second inflationary phase

To realize the SU(2) sector as the Standard Model $\mathrm{SU_L}(2)$ sector, we consider gauge field couplings $g = \mathcal{O}(0.1)$. In our simulation, we examine two cases: $g = 0.1$ (runs A1, A2, B, and C1-3) and $g = 0.65$ (runs D and E). The backreaction bound given in eq. (2.17) suggests that the value of m_Q should be less than 1.3 for the $g = 0.65$ case and less than 2.4 for the $g = 0.1$ case to avoid backreaction of the tensor perturbations of the SU(2) gauge fields on its background evolution. It is important to note that, even if the value of m_Q is below the backreaction bound initially, backreaction may still become important at a later epoch during inflation (see the run $\mu3$ in ref. [104]). We also consider $m_Q > \sqrt{2}$ to avoid instability of the scalar perturbations of the SU(2) sector. Therefore, for the case of $g = 0.65$, backreaction will be significant from the beginning since $m_Q > \sqrt{2}$ already lies within the backreaction regime. However, for the case of $g = 0.1$, by properly choosing a value of m_Q smaller than 2.6, backreaction will not be important initially, but can become significant at a later stage in the evolution.

For the numerical simulations, we use the Pencil Code [119] and solve the background equations (2.6), (2.7), (2.10), (2.25)–(2.28) with perturbation equations (2.23)–(2.24). The simulations are performed in cosmic time. Similarly as in ref. [104], we set the initial conditions for the real and imaginary parts of the perturbation variables as

$$T_{R,L} = \frac{1}{\sqrt{2k}}e^{ik/a_iH_i}, \quad \partial_t T_{R,L} = -\frac{i}{a_i}\sqrt{\frac{k}{2}}e^{ik/a_iH_i}, \tag{3.3}$$

(similarly for $\psi_{R,L}$) with $a_i = 1$. The contributions from quantum vacuum fluctuations of $T_{R,L}$ in the calculation of the backreaction integrals in eqs. (2.27) and (2.28) are discarded by setting $|T_{R,L}|^2$ to zero when $|T_{R,L}|^2 < 1/2k$. In our simulations, we have n_k points of k in the range

$$n_{\rm min} \le \ln(k/a_iH_i) \le n_{\rm max}. \tag{3.4}$$

The n_k points are chosen such that they are distributed uniformly in $\ln k$ and $n_k = 2048$ for all our simulations. The values of $n_{\rm min}$ and $n_{\rm max}$ are provided in table 1 for each run.

JCAP12(2024)057

We show the background evolution of the gauge field VEV Q and axion field χ/f in the upper left and right panels of figure 1, respectively. We set $(\pi - \chi/f) < 0.1$ initially, so that the axion and gauge field VEV relax to their respective minima (before or) close to the end of inflation. The solid orange and dashed blue curves correspond to the quadratic and α-attractor inflationary models, respectively. For $g = 0.1$ and $m_Q \simeq 2.37$, the backreaction of the perturbations is significant, which forces Q to settle into the negative attractor solution (2.29)–(2.30) and reduces the velocity of the χ field, as discussed in refs. [104, 105]. As χ approaches a minimum of its potential, Q tends to zero and remains there, transitioning from a chromo-natural attractor into the trivial vacuum of the theory. The transition to zero is occurring smoothly for all the runs considered; see figure 1 with solid orange curve (run B, quadratic inflation), dashed blue (run C1, α-attractors), dot-dashed green (run A1, const H), and dot-dashed purple (run A2, const H). For the "const H" runs, the Hubble parameter is constant during inflation, but we choose a different initial value for the axion field in each run; see table 1. The initial parameters are such that the end of inflation occurs at $N = 61.4$ for the quadratic model and $N = 58.2$ for the α-attractor model. The end of inflation is defined as the time when the first slow-roll parameter ϵ_H (2.14) reaches unity. In the lower panels of figure 1, we show the time evolution of ϵ_H (bottom left panel) and $m_Q\xi$ (bottom right panel), defined by eq. (2.16). During inflation, when the Hubble parameter is approximately constant, we see that $m_Q\xi \simeq -1$ and the system stays at the backreaction-supported attractor with $Q < 0$; see appendix D of ref. [104]. When the axion relaxes into a minimum of its potential, $m_Q\xi$ vanishes.

Tensor perturbations of the gauge field will eventually seed magnetic fields. Hence, it is crucial to investigate the dynamics of perturbations as Q approaches zero. We show the evolution of gauge field perturbations $T_{R,L}$ in figure 2 for three different values of the comoving wave number k. Before the transition of $Q \to 0$, the evolution of T_R for the super-horizon modes is such that $\sqrt{2k}\, xT_R(x)$ remains (roughly) constant in time,[6] where $x \simeq k/(aH)$. This is derived through the equation for T_R

$$\partial_x^2 T_{R,L} + \left(1 + \frac{2}{x^2} m_Q\xi\right) T_{R,L} \simeq 0\,; \tag{3.5}$$

see appendix D of ref. [104] for more details. At the backreaction-supported attractor $m_Q\xi \simeq -1$, and by considering the super-horizon regime where $x \simeq k/aH \ll 1$, we see that $T_{R/L} \propto 1/x$ and thus the combination $xT_{R/L}$ remains constant as long as the system follows the backreaction-supported attractor. We can define the (almost) constant value of $xT_{R/L}$ during the attractor through

$$\sqrt{2k}\, xT_R = c_1(k) \tag{3.6}$$

where the constant c_1 is different for each wave number k.

Before transitioning to the next section and discussing the evolution of perturbations around the end of inflation, we demonstrate the possibility of a second inflationary phase. If the χ field is initialized such that its initial value is far from the one corresponding to the

[6] The evolving Hubble scale near the end of inflation leads to a $m_Q\xi$ deviating slightly from -1 and thus xT_R being almost constant but not exactly so.

JCAP12(2024)057

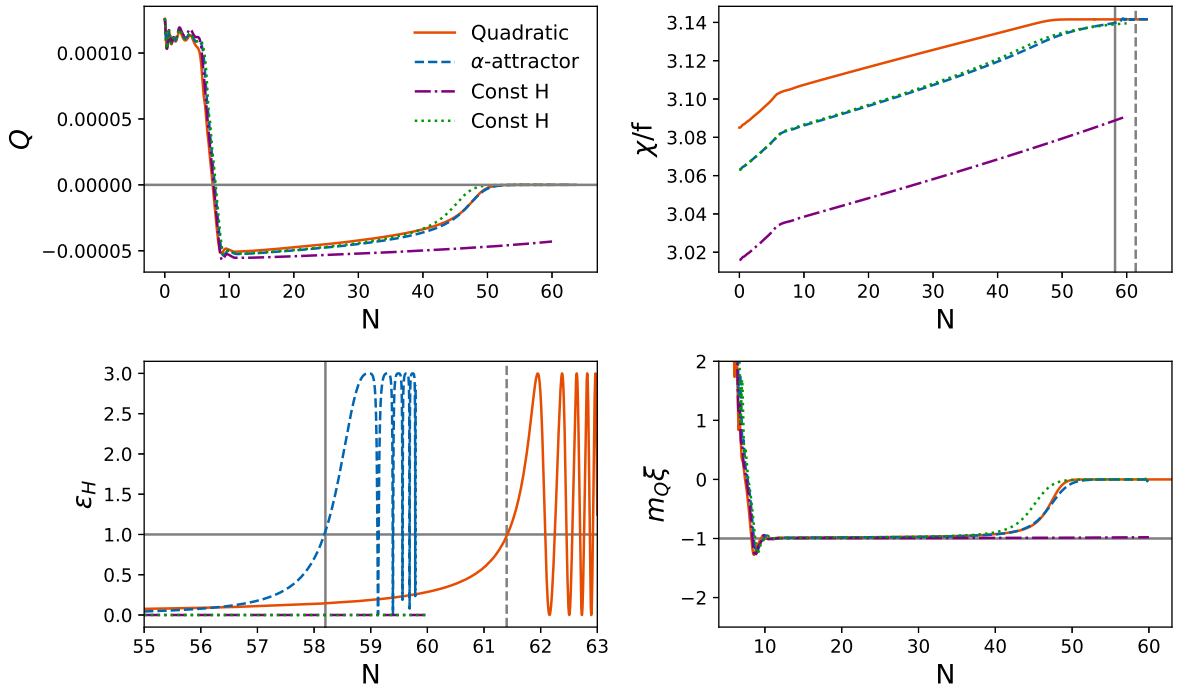

Figure 1. The evolution of gauge field VEV Q (top left), axion field χ/f (top right), the first slow-roll parameter ϵ_H (bottom left) and the combination $m_Q\xi$ (bottom right) with respect to the number of e-folds N for different simulations. The solid orange curve corresponds to (run B, quadratic inflation) and the dashed blue to (run C1, α-attractors). The dot-dashed green (run A1, const H) and dot-dashed purple (run A2, const H) curves relate to scenarios where H remains constant during inflation but with different initial values of χ/f: smaller for run A2 and bigger for run A1. The solid and dashed grey grid lines correspond to the end of inflation for runs C1 and B, respectively. The color coding is the same for the whole panel. The parameters for each run are shown in table 1.

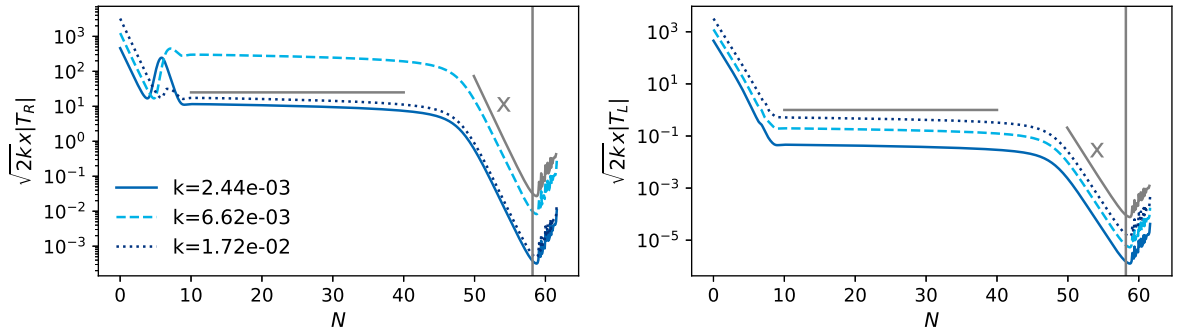

Figure 2. The evolution of tensor perturbations of gauge field $T_{R,L}$ with respect to the number of e-folds N for there different k-values for run (C1, α-attractors). The grey vertical lines represent the end of inflation. The two grey line segments designate a constant value and a function proportional to x. The values of k shown in the legend are normalized by $M_{\rm pl}$.

JCAP12(2024)057

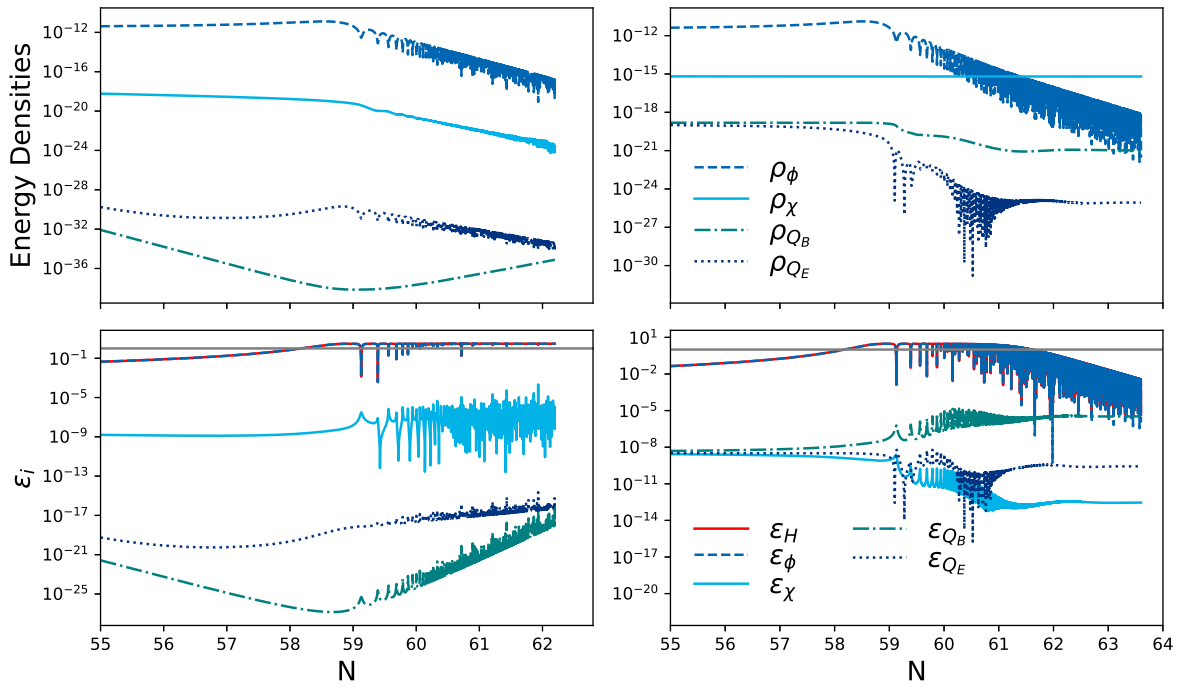

Figure 3. The upper panels show the evolution of energy densities of the inflaton field ρ_ϕ (dashed blue curve), axion field ρ_χ (solid cyan curve), and SU(2) gauge field (dotted dark blue curve for ρ_{Q_E} and dot-dashed green for ρ_{Q_B}) for the α-attractor potential and runs C1 (left panel) and F (right panel). For the run C1 the axion reaches a minimum of its potential before the end of inflation. For run F we chose a smaller initial value of the axion field such that a minimum of axion potential is not reached. The latter case leads to the second phase of inflation, dominated by the chromo-natural sector. The lower panels show the evolution of the first slow-roll parameter ϵ_H, along with the different contributions defined in eq. (2.14).

minimum of its potential ($\chi/f = \pi$), the axion field will not reach its minimum by the end of inflation and the total energy density of the χ field will remain dominated by its potential energy. Since the energy density of the inflaton field decreases after the end of inflation, the total energy density of the universe will eventually be dominated by the almost constant potential energy of the χ field. At this point, the system will enter a second inflationary era, dominated by the potential energy of the axion, similarly to chromo-natural inflation.[7]

Figure 3 shows the evolution of the energy densities of the inflaton field ρ_ϕ (dashed blue curves), axion field ρ_χ (solid cyan curves), and the electric ρ_{Q_E} (dotted dark blue curves) and magnetic ρ_{Q_B} (dot-dashed green curves) components of the background energy density of the SU(2) field, defined in equation (2.13). Here we use the α-attractor potential and runs C1 (left panel) and F (right panel) from table 1. In the lower part of this figure, we show the evolution of the first slow-roll parameter, ϵ_H, along with the different contributions as defined in eq. (2.14) for these runs.

[7]Interestingly though, at least initially, the first slow-roll parameter ϵ_H is strongly affected by the oscillating field ϕ and thus exhibits itself oscillations on top of an average value of $\epsilon_H < 1$. When these die out, we expect this second inflationary stage to be identical to "standard" chromo-natural inflation.

JCAP12(2024)057

For run C1, the initial value of the χ field is $0.975\pi f$, and the axion reaches a minimum of its potential before the end of inflation, as indicated by the dotted blue curves in figure 1. For run F, we chose a smaller initial value of the χ field (further away from the minimum and higher up the potential), $\chi/f = 0.9\pi$. For this run, the χ does not reach a minimum of its potential by the end of inflation and the total energy density of the χ field remains dominated by its potential energy. Around $N \approx 62$, the total energy budget of the universe becomes dominated by the potential energy of the χ field, ushering a second inflationary stage, as shown by the evolution of ϵ_H for run F. For the remainder of this work, we choose initial parameters for the background axion and gauge field that preclude the existence of a prolonged secondary inflationary stage.

3.3 Evolution of gauge field modes with vanishing VEV

In this section we examine the evolution of the gauge field modes T_R when the gauge field VEV Q approaches zero. When $m_Q\xi$ becomes zero, eq. (3.5) in terms of conformal time defined as $d\tau = dt/a$ reduces to,

$$\partial_\tau^2 T_R + k^2 T_R = 0. \tag{3.7}$$

The general solution of the above equation is

$$T_R = d_1 \sin k\tau + d_2 \cos k\tau. \tag{3.8}$$

By matching this solution to the solution with $\sqrt{2k}\, xT_R = c_1(k)$ at the transition of Q from the backreaction-supported attractor to zero (assuming this is fast enough) in the superhorizon limit ($-k\tau \ll 1$), we obtain the following expression for T_R

$$T_R \approx \frac{c_1(k)}{\sqrt{2k}} \frac{a_T^2 H^2}{k^2} \left[\sin k(\tau - \tau_T) + \frac{k}{a_T H} \cos k(\tau - \tau_T) \right], \tag{3.9}$$

where a_T denotes the value of the scale factor at the time when Q transitions from the backreaction-supported attractor to zero during inflation, and $\tau_T = -1/(a_T H)$.

Let us pause momentarily to discuss this transition. Figure 2 clearly shows two distinct types of behavior for the gauge field modes T_R. For $m_Q\xi \simeq -1$, $T_R \propto 1/x$ and for $m_Q\xi \simeq 0$, $T_R \sim$ const. By using these two simple power-law behaviors, we can define a "knee" in the corresponding plot of T_R, which for figure 2 occurs roughly at $N = 45$ e-folds. We define the scale-factor at this time as a_T. The analysis presented here uses the assumption that this transition is instantaneous. As we see in figure 1, the transition of $m_Q\xi$ from -1 to 0 can take a few e-folds. However, the introduction of a_T allows us to understand the behavior without unnecessarily complex calculations. Furthermore, in the estimation of the late-time magnetic field that appears in the next section, we use the value of T_R at the end of inflation, as extracted from our full numerical simulation. Therefore we keep the transition scale-factor a_T as a useful notation, keeping in mind the limitations of this approximation.

In the superhorizon limit ($k\tau \ll 1$) the cosine part of eq. (3.9) gives the dominant contribution and the mode function can be approximated as

$$T_R \approx \frac{c_1(k)}{\sqrt{2k}} \frac{a_T H}{k}. \tag{3.10}$$

JCAP12(2024)057

The energy density of T_R after $Q \to 0$ (equivalently $m_Q \to 0$) is written in terms of conformal time as

$$\rho_{T_R} = \frac{1}{a^4} \int \frac{d^3k}{(2\pi)^3} \frac{1}{2} \left(|\partial_\tau T_R|^2 + k^2 |T_R^2| \right). \tag{3.11}$$

By substituting T_R from eq. (3.9) into this expression, we get

$$\rho_{T_R} = \frac{1}{4} \left(\frac{a_T}{a} \right)^4 H^4 \int \frac{d\ln k}{(2\pi)^3} |c_1(k)|^2 \left(1 + \left(\frac{k}{a_T H} \right)^2 \right). \tag{3.12}$$

From the above expression, we conclude that the energy density of T_R decays as $1/a^4$ after Q becomes zero, as expected for a radiation degree of freedom in an expanding universe.

When $Q \to 0$ before the end of inflation, there is a period during inflation where T_R is almost constant until the transition to $Q = 0$ occurs at a_T. Figure 1 shows that Q approaches zero between 40 to 50 e-folds for run C1 (the dashed blue curve). Consequently, $\sqrt{2k}\, xT_R$ starts decreasing as x decreases, as shown in figure 2. However, if we initially choose a smaller value of χ/f and a smaller μ value to maintain the same value of m_Q, the transition of Q to zero happens later compared to run C1. We demonstrate this in appendix A. Therefore, for fixed m_Q and g values, the largest possible value of T_R at the end of inflation is achieved when the transition of Q to zero happens very close to the end of inflation. In this case, $\sqrt{2k}\, xT_R$ will remain constant until the end of inflation. In section 4 we further investigate the implications for magnetogenesis when Q vanishes at different times during inflation.

4 Post inflationary gauge field evolution and magnetic field generation

In this section, we study the evolution of gauge field perturbations after the end of inflation. For the evolution after inflation, we assume that reheating occurs instantaneously, after which the universe transitions into a radiation-dominated era. This can be accomplished for example through tachyonic preheating of the inflaton sector. An intriguing possibility is the identification of the inflaton as a pseudo-scalar field (axion) and the natural addition of a $\phi F\tilde{F}$ coupling of the axion-inflaton to U(1) gauge fields. Since it has been shown [33, 120] that Chern-Simons couplings to U(1) fields can preheat the universe after inflation instantaneously, while leaving the inflationary history largely unaffected (for a proper choice of parameters), this presents a unifying picture of our model, where two axions are coupled to different gauge sectors and one (the inflaton) dominates the energy density and thus drives inflation.

As discussed in the previous section, when Q approaches zero, the solution for T_R is given by eq. (3.9). This solution indicates that T_R remains almost constant when a particular wavelength is much larger than the size of the Hubble horizon and begins oscillating once the mode re-enters the horizon. In the superhorizon limit, the constant value of T_R is given by eq. (3.10), which can also be expressed as

$$T_R \approx \frac{c_1(k)}{\sqrt{2k}} \frac{a_T}{a_e} \frac{a_e H}{k}. \tag{4.1}$$

Here, a_e denotes the value of the scale factor at the end of inflation, and a_T/a_e accounts for the suppression in the value of T_R, depending on how early Q reaches zero before the

JCAP12(2024)057

end of inflation. As $m_Q\xi$ remains zero, the evolution of T_R after inflation follows eq. (3.7). Therefore, in the post-inflationary era, T_R can be written as an oscillatory function of conformal time for modes larger than the Hubble size, while its energy density decays like radiation, as described by eq. (3.12).

Having determined the evolution of the gauge field modes after inflation, we are ready to consider their evolution through the electroweak phase transition.

4.1 Magnetogenesis

At the electroweak era, a component of the SU(2) field transforms into the electromagnetic field. The relation between the electromagnetic field A_μ, the SU(2) field W^a_μ, and the hypercharge field B_μ is given by

$$A_\mu = W^3_\mu \sin\theta_W + B_\mu \cos\theta_W, \tag{4.2}$$

where θ_W is the weak mixing angle (Weinberg angle). Neglecting the contribution of B_μ and using $\sin\theta_W \sim 0.5$, we get

$$A_\mu \approx 0.5 W^3_\mu. \tag{4.3}$$

Without loss of generality we associate the perturbations as $\delta W^0_3 = 0$, $\delta W^3_i = a t_{i3}$. Assuming that tensor perturbations of the SU(2) gauge field give the dominating contribution after inflation, from eqs. (2.18), (2.19) and (2.22) we arrive at

$$|A_i|^2 = \frac{1}{4}\left(|T_L|^2 + |T_R|^2\right). \tag{4.4}$$

In terms of the vector potential, A_i, the magnetic energy spectrum is given by (see eq. (17) in ref. [121]),

$$\Delta_{\rm B}(k) = \frac{1}{(2\pi)^2}\frac{k^5}{a^4}|A_i|^2. \tag{4.5}$$

Here, $\Delta_{\rm B}$ represents the magnetic energy spectrum per logarithmic wave number interval and is defined such that the magnetic energy density is $\rho_B \equiv \langle B^2/2\rangle = \int d\ln k\, \Delta_{\rm B}(k)$. Using eqs. (3.9) and (4.4), we arrive at the following expression for the magnetic energy spectrum at the EW epoch

$$\Delta_{\rm B}(k) = \frac{1}{(2\pi)^2}\frac{k^5}{a^4}\frac{1}{4}\left(|T_L|^2 + |T_R|^2\right) \sim \frac{1}{(2\pi)^2}\frac{a_e^4 H_e^4}{a^4}\left(\frac{a_T}{a_e}\right)^4 \frac{1}{8}|c_1|^2 \sin^2 k(\tau - \tau_e). \tag{4.6}$$

Here H_e represents the value of the Hubble parameter at the end of inflation. For subhorizon modes ($k\tau \gg 1$), the typical value of $\sin^2 k(\tau-\tau_e)$ can be approximated by 1/2. Furthermore, by normalizing $\Delta_{\rm B}(k)$ with the total energy density of the universe at the end of inflation, $\rho_e = 3H_e^2 M_{\rm pl}^2$, we can write

$$\frac{\Delta_{\rm B}(k)}{\rho_e} \sim \frac{a^4}{3H_e^2 M_{\rm pl}^2 a_e^4}\frac{1}{16(2\pi)^2}\frac{a_e^4 H_e^4}{a^4}\left(\frac{a_T}{a_e}\right)^4 |c_1|^2 = \frac{1}{48(2\pi)^2}\left(\frac{H_e}{M_{\rm pl}}\right)^2\left(\frac{a_T}{a_e}\right)^4 |c_1|^2. \tag{4.7}$$

JCAP12(2024)057

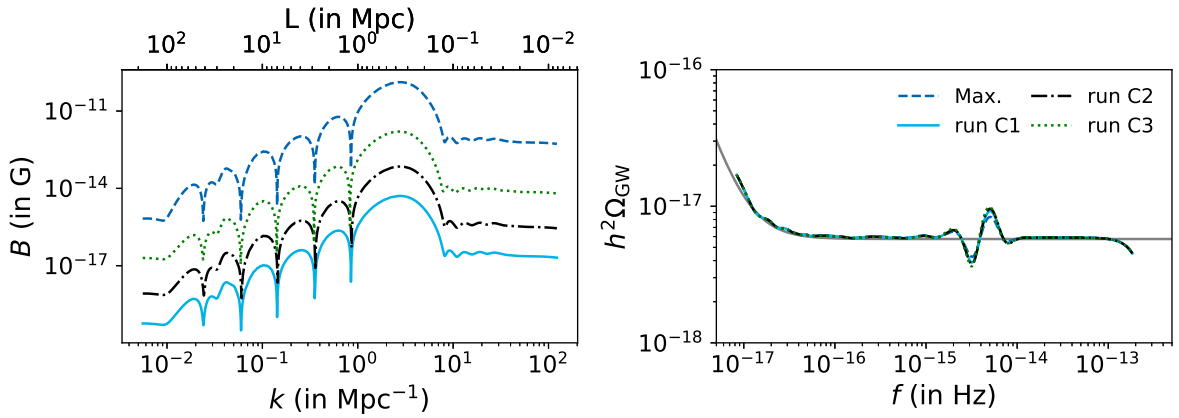

Figure 4. The left panel of this figure shows the magnetic field amplitude B at the present epoch given by eq. (4.8) with respect to the wave number and coherent length. We use the α-attractor potential and runs C1 (solid cyan curve), C2 (dot-dashed black) and C3 (dotted green) from table 1. The dashed blue curve corresponds to run C1 with $a_T/a_e = 1$, which implies that $\sqrt{2k}\,xT_R$ for all the super-Hubble modes remains constant until the end of inflation. The evolution of Q and χ/f for these runs is shown in figure 6 in appendix A and as a dashed blue curve in figure 1 for run C1. The right panel shows the corresponding gravitational wave spectral energy density fraction with the same color coding and its vacuum contribution (estimated using eq. (4.14)) in the grey curve.

The above expression implies that the magnetic energy spectrum is proportional to $|c_1|^2$. Using the value of the radiation energy density at the present epoch to be $\sim (3\,\mu\text{G})^2$, the magnetic field strength at its peak wave number becomes

$$B \approx \sqrt{2\Delta_{\rm B}(k)\big|_0} = 9.7\times10^{-8}\frac{H_e}{10^{-6}M_{\rm pl}}\left(\frac{a_T}{a_e}\right)^2|c_1|\ \mu\text{G}. \tag{4.8}$$

We use equation (4.8) to compute the magnetic field strength at the present epoch, using the value of $(a_T/a_e)^2|c_1|$ obtained from the simulation at the end of inflation, as discussed earlier. The resulting amplitude with respect to the wave number k and the corresponding length scale are shown in the left panel of figure 4 for runs C1–C3. The peak value of the obtained magnetic field strength is 5.3×10^{-15} G, 7.4×10^{-14} G, and 1.6×10^{-12} G for the runs C1 (solid cyan curve), C2 (dot-dashed black curve), and C3 (dotted green curve), respectively. The dashed blue curve represents the case where we used $a_T = a_e$ in eq. (4.8) for run C1 and the corresponding magnetic field strength is 1.3×10^{-10} G. This occurs when the initial value of χ is fine-tuned, so that $Q \to 0$ very close to the end of inflation. As can be inferred from table 1, such fine-tuning requires choosing the initial value of χ/f at the 0.1% level. Since this is not necessary for the viability of our model, we do not attempt to provide this exact value. Therefore, to obtain the magnetic field strength shown in the dashed blue curve, we use the value of $|c_1|$ from run C1 at $N = 30$, where $x|T_R|$ is in the regime where it is almost constant in time.

The magnetic energy spectra peak at a length scale of approximately 0.4 Mpc for these cases with amplitudes that satisfy the lower bound from blazar observations, as shown in figure 5 with black stars. The red star on the figure represents the case with the larger value of m_Q. In that situation the backreaction effects become important earlier and the

JCAP12(2024)057

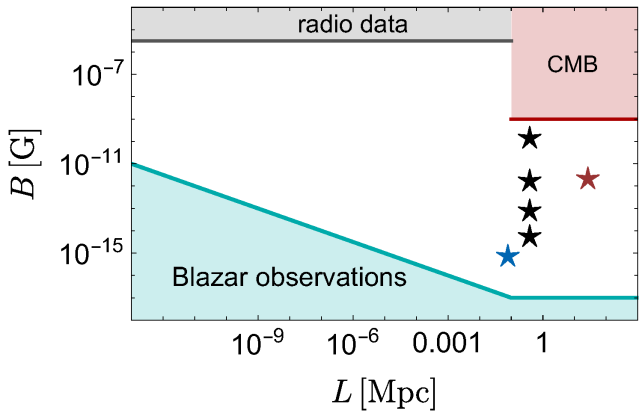

Figure 5. Bounds on intergalactic magnetic fields adapted from reference [122]. The light blue-shaded region shows the lower bound inferred from blazar observations [12], the red-shaded upper bound shows Planck Collaboration analyses [123] and the light-grey shaded upper bound are conservative limits from radio data [124] and theoretical estimates [18]. By black stars we illustrate the magnetic field amplitudes from figure 4 and the red and blue stars refer to corresponding peaks of the red-dashed and blue curves in figure 7.

system transitions to the backreaction-supported attractor shortly after the start of inflation, moving the peak of magnetic energy spectra to larger scales, as discussed in appendix B (see the corresponding red-dashed curve in figure 7). For smaller m_Q values, this transition happens later, pushing the magnetic field peak value to smaller scales, as represented by the blue star and corresponding to the blue curve in figure 7. The resulting amplitude of the magnetic field depends on the initial value of parameter m_Q as well on how close to the end of inflation the gauge field VEV converges to zero. From figure 5 it follows that the magnetic fields produced during spectator chromo-natural inflation can potentially explain the presence of the magnetic fields in the intergalactic medium.

In figure 4, the wave number k at the present epoch is computed as

$$k = e^{-(N_e - N_k)} k_H, \tag{4.9}$$

where N_e and $N_k = \ln(k/H)$ represent the total number of e-folds during inflation and the number of e-folds at which the wave number k exits the Hubble horizon during inflation, respectively, and k_H represents the present-day value of the wave number corresponding to the Hubble size at the end of inflation and is given by

$$k_H = \frac{a_e}{a_0} H = 2.3 \times 10^{22}\,\mathrm{Mpc}^{-1} \left(\frac{\mathrm{H}}{10^{-6}\mathrm{M_{pl}}}\right)^{1/2}. \tag{4.10}$$

In the above expression, we assumed an adiabatic evolution of the universe,

$$\frac{a_e}{a_0} = \left(\frac{g_{0s}}{g_{rs}}\right)^{1/3} \frac{T_0}{T_r} = 5.96 \times 10^{-29} \left(\frac{g_{0s}}{3.94}\frac{106.75}{g_{rs}}\right)^{1/3} \frac{T_0}{2.73\mathrm{K}} \left(\frac{10^{-6} M_{\mathrm{pl}}}{H}\right)^{1/2}, \tag{4.11}$$

where g_{rs} and g_{0s} denote the effective degrees of freedom in the entropy at the end of inflation and the present epoch, respectively. We estimate the reheating temperature, T_r, by assuming instantaneous reheating using $3H^2 M_{\mathrm{pl}}^2 = (\pi^2/30) g_r T_r^4$.

JCAP12(2024)057

Furthermore, we calculate the gravitational wave spectral energy density fraction, $\Omega_{\rm GW}h^2$ defined as

$$h^2\Omega_{\rm GW}(k) = \frac{3}{128}h^2\Omega_{\rm rad}\mathcal{P}_h^{\rm tot}(k)\left[\frac{1}{2}\left(\frac{k_{\rm eq}}{k}\right)^2 + \frac{16}{9}\right]. \tag{4.12}$$

Here, $h^2\Omega_{\rm rad} \simeq 2.47 \times 10^{-5}$ represents the current radiation density fraction, and $k_{\rm eq} \simeq 1.3 \times 10^{-2}\,{\rm Mpc}^{-1}$ is the wave number corresponding to the Hubble horizon at matter-radiation equality. The parameter h is defined such that $H_0 = 100\,h\,{\rm km\,s^{-1}\,Mpc^{-1}}$, where H_0 is the Hubble parameter at the present epoch. To express $\Omega_{\rm GW}$ in terms of frequency, f instead of wave number, k, we use $f \simeq 1.5 \times 10^{-15}(k/1\,{\rm Mpc}^{-1})\,{\rm Hz}$. In the expression (4.12) $\mathcal{P}_h^{\rm tot}(k)$ is the total power spectrum of sourced gravitational waves by the tensor perturbations of the SU(2)-gauge field, defined as

$$\mathcal{P}_h^{\rm tot}(k) = \frac{2H^2}{\pi^2 M_{\rm pl}^2}\sum_{s=L,R}\left|\sqrt{2k}\left(\frac{k}{aH}\right)\lim_{k/aH\to 0}\psi_{(s)}\right|^2 \tag{4.13}$$

for the sourced contribution from the tensor perturbations of the SU(2)-gauge field. The vacuum contribution of tensor the metric perturbations is

$$\mathcal{P}_h^{\rm vac}(k) = \frac{2H^2}{\pi^2 M_{\rm pl}^2}. \tag{4.14}$$

We show the gravitational wave spectral energy density fraction and its comparison to vacuum contribution in the right panel of figure 4. We can see that oscillations in T_R produce oscillations in $\Omega_{\rm GW}h^2$, but for the runs C1–C3, the amplitude of gravitational waves is small and unobservable in the upcoming surveys. For larger values of m_Q, the amplification is significant. We show this in appendix B.

4.2 Comparison with magnetogenesis from axion-U(1) inflation

It is important to compare the underlying physics of magnetogenesis from axion-U(1) inflation [23, 33, 36, 125] to our current work. In the case of axion-U(1) inflation, one of the gauge field modes is amplified due to the coupling between the axion and U(1). The strength of this amplification depends on the velocity of the axion, and the axion-gauge coupling — a faster-rolling axion results in more rapid growth of the gauge field. As the axion's velocity becomes maximal near and after the end of inflation, the gauge field modes with wavelength comparable to the horizon at this time experience maximum amplification. In practice, the most efficient amplification of gauge fields occurs during preheating, where it was shown in ref. [33] that the inflaton can transfer the entirety of its energy density to gauge fields, leading to a magnetic field strength $B^2 \sim M_{\rm Pl}^2H^2$. Consequently, a spectrum is obtained that peaks around the Hubble horizon scale near the end of inflation with large amplitude.

These fields are largely helical[8] and undergo an inverse cascade, leading to typical length scales on the order of parsecs, with a strength of around $10^{-13}\,{\rm G}$ [33]. The wave number modes corresponding to present-day length scales of approximately 1 Mpc leave the horizon

[8]The gauge fields would be exponentially close to being totally helical, but non-rescattering during preheating alleviates part of the helicity [33].

JCAP12(2024)057

about 10 e-folds into inflation. However, their amplitude continues to decay even after crossing the horizon, resulting in a very small magnetic field at the end of inflation, leading to tiny magnetic field strength at those scales.

In contrast, the dynamics in the case of inflation with a (spectator) axion-SU(2) sector is quite different due to the existence of the backreaction-supported attractor. Since the magnetic field arises from a component of the SU(2) gauge field's tensor perturbations, the magnetic field spectrum is related to the tensor perturbation spectrum. The tensor perturbation spectrum peaks roughly at a scale corresponding to the Hubble horizon scale around the epoch when Q transitions from the initial spectator chromo-natural attractor to the backreaction-supported attractor. As an example, in the case of runs C1–C3, this transition occurs around 10 e-folds from the start of inflation; see figure 1. Therefore the modes which exit the Hubble horizon around this time experience maximum amplification. The backreaction from these perturbations becomes important and the system transitions to the backreaction-supported attractor. During this stage, $m_Q\xi \simeq -1$, which leads to a constant amplitude of $\sqrt{2k}\, xT_R$ during the super-horizon evolution, with roughly no decay until Q reaches zero. Modes that exit the horizon during the backreaction-supported attractor phase do not undergo much amplification due to the small value of m_Q. Referring again to runs C1–C3, backreaction becomes significant after around 10 e-folds, and the modes that exit around this time, or earlier, correspond to a length scale of the order of 1 Mpc at the present epoch. This is why the magnetic field spectrum shown in the figure 4 peaks at megaparsec scales. Simply put, the Abelian case relies on extremely efficient energy transfer to gauge fields, albeit at small scales, whereas the non-Abelian case relies on the non-decay of gauge fields during the backreaction-supported attractor, allowing for much larger correlation lengths, albeit with weaker field strength.

It is instructive to compare the dynamics of the backreaction-supported attractor with the Anber-Sorbo solution [57], which describes the homogeneous backreaction regime in axion-U(1) inflation and has recently been shown to be unstable [73]. While in both U(1) and SU(2) cases the backreaction is treated similarly through a homogeneous Hartree-type approximation, the dynamics differ significantly due to the presence of a non-zero VEV in the non-Abelian case. The Anber-Sorbo solution for the U(1) case hinges on the continuous production of gauge field modes with ever increasing comoving wave number and thus a change in their growth rate can destabilize it. Conversely, in the SU(2) case, the primary contribution to the backreaction integrals arises only from a fixed range of comoving wave numbers, which allows for a stable solution. We refer the interested reader to appendix D of ref. [104] for a detailed discussion on this comparison. Though the backreaction-supported attractor in the non-Abelian case breaks down close to the end of inflation, where the solution smoothly converges to zero, it provides an excellent approximation during inflation.

4.3 Magnetic mass effects

Non-Abelian gauge bosons in a high-temperature plasma, as the one present in the early universe, can acquire an additional mass, dubbed "magnetic mass". In the previous discussion, we did not consider effects coming from a magnetic mass, which is typically considered to be of the form $m_{\rm mag} \propto g^2 T$ [126], where T is the temperature of the universe and g is the

JCAP12(2024)057

gauge-field coupling. The effect of the additional mass term can be estimated using [127]

$$\partial_\tau^2 T_R + \left(k^2 + a^2 m_{\rm mag}^2\right) T_R \simeq 0. \tag{4.15}$$

However, a field with a mass proportional to the temperature behaves like radiation, meaning that the magnetic field scaling shown in section 4 is still valid. Since in the radiation-dominated era $a \propto \tau$ and $T \propto \sqrt{H} \propto \frac{1}{\tau}$, leading to $a^2 m_{\rm mag}^2 = \text{const}$, the magnetic mass will modify the oscillation frequency of perturbations, leaving the amplitude unchanged (except possible effects from the time-varying initial creation of the thermal plasma).

An interesting analogy of the EWPT is that of a superconductor. We can imagine the super-horizon gauge fields before the EWPT as a magnetic field permeating a superconductor with a temperature larger than the superconducting phase transition. If one lower the temperature, when the solid turns into a superconductor, the previously homogeneous magnetic field will break into filaments surrounded by current vortices. Similar formation of magnetic structures, including flux tubes, filaments and vortices, also occurs when magnetic fields interact with a plasma. It is intriguing to further explore the details of the magnetic field evolution through the EWPT. While it is computationally challenging, progress in simulating structures in the full electroweak theory has been made (see e.g. [128]) and such a simulation is necessary to probe whether magnetic fields produced in this model will acquire spatial patterns when the Higgs relaxes to its VEV and the SU(2) fields get partially transformed into electromagnetic fields.

5 Summary and discussion

We have explored the consequences of spectator chromo natural inflation (SCNI), where the non-Abelian gauge field is identified with the $\mathrm{SU(2)_L}$ sector of the Standard Model. This fixes the gauge coupling to be large $g \gtrsim \mathcal{O}(0.1)$, bringing the backreaction contribution from tensor perturbations to be comparable to other terms in the background equations of motion. The system necessarily flows into the recently discovered backreaction-supported attractor that appears in this regime [104].

In our previous work [104], we studied the evolution of the SCNI sector during inflation under the assumption of a constant Hubble parameter and discovered a new type of dynamical attractor, supported by the backreaction of gauge field fluctuations on the background trajectory. Here, we relaxed this assumption and analyzed the dynamics of the axion-gauge field system until the end of inflation, using quadratic and alpha-attractor potentials to model the background evolution of the inflaton. We stressed an important point, which was overlooked so far in the literature. In these models there is a possibility for a second inflationary stage, after the inflaton rolls to its potential minimum, driven by the energy density of the axion field of the SCNI sector. To avoid this case, we focused on cases where the initial value of the axion field is chosen such that it reaches the minimum of its potential before the end of inflation. When the axion field approaches a minimum of its potential, the gauge field VEV smoothly transitions to zero, and the tensor perturbations of the gauge fields begin to red-shift as expected for gauge fields in an FRW spacetime. During the EWPT, part of the tensor perturbations of the SU(2) gauge field get transformed into the

JCAP12(2024)057

electromagnetic part of the broken $SU(2)_L \times U(1)_Y$ sector. The electric component of the fields will be quickly damped (typically within one Hubble time) due to the large conductivity of the Universe. However, the magnetic component will remain frozen, providing a viable origin for the presence of magnetic fields in the intergalactic medium. The obtained magnetic field at the present epoch depends on the axion-SU(2) model parameters. For one set of parameter choices presented here, we found that the magnetic fields have a strength of 5×10^{-15} G with a coherence length of approximately 0.4 Mpc at the present epoch. This is above the lower bound on the strength of the magnetic field in the intergalactic medium inferred from GeV observations of blazars.

Given the intriguing dynamics and important phenomenology of this model, several avenues for future work arise. So far, we have analyzed the dynamics of the axion-SU(2) system using the linear evolution equations for the gauge field modes. It was recently shown [106] that accounting for gauge field self-interactions and axion-gauge field non-linear couplings leads to bounds on the parameters of the model, so that a perturbative description of the theory is valid. Interestingly, these bounds on the parameter space of the theory are comparable to the edge of the strong backreaction regime. It is thus necessary to perform a full numerical computation to accurately determine the exact perturbativity bounds and their competition with the strong backreaction regime. Moreover, our analysis neglects spatially dependent backreaction effects, that have been shown to have a strong impact on the overall dynamics close to the end of inflation in the Abelian case [74]. Performing lattice simulations would be a natural next step to explore the non-linearities in axion-SU(2) gauge field dynamics. Finally, the detailed evolution of the produced SU(2) gauge fields through the EWPT and the possibility of the creation of magnetic field filaments, akin to the case of a superconductor, is beyond the scope of our present calculation. Further analysis of these exciting aspects is left for future work.

Acknowledgments

We thank G. Dvali, T. Fujita, K. Kamada, A. Long, K. Mukaida, K. Subramanian and T. Vachaspati for useful discussions on the evolution of non-Abelian fields. A.B., O.I. and E.I.S. acknowledge the hospitality of the Bernoulli Center during the workshop "Generation, evolution, and observations of cosmological magnetic fields", where part of this work was conducted and presented. A.B. was supported in part by the Swedish Research Council (Vetenskapsrådet) under Grant No. 2019-04234, the National Science Foundation under Grants No. NSF PHY-2309135 and AST-2307698, and the NASA ATP Award 80NSSC22K0825. The work of O.I. was supported by the European Union's Horizon 2020 research and innovation program under the Marie Skłodowska-Curie grant agreement No. 101106874. R.S. was supported by the Czech Science Foundation (GAČR), project 24-13079S. We acknowledge the allocation of computing resources provided by the Swedish National Allocations Committee at the Center for Parallel Computers at the Royal Institute of Technology in Stockholm.

Data availability. The source code used for the numerical solutions of this study, the Pencil Code, along with the module `special/axionSU2back` used in the present study, are freely available at https://github.com/pencil-code/pencil-code/. The numerical data and input files are available on Zenodo; see ref. [129].

JCAP12(2024)057

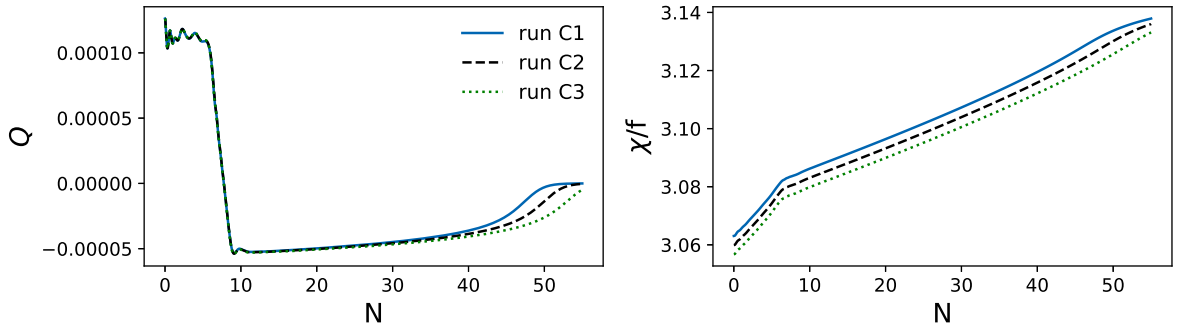

Figure 6. The evolution of the Q (left panel) and χ/f (right panel) for the runs C1 (solid blue curves), C2 (dashed black curves), and C3 (dotted green curves).

A Different initial values of χ/f and μ

In this section we show the evolution of the axion-SU(2) system for different initial values of χ/f and μ, while keeping the initial values of m_Q constant for a fixed value of g. In figure 6 we illustrate the evolution of Q and χ/f for runs C1 (solid blue curves), C2 (dashed black curves) and C3 (dotted green curves). The initial parameters for these runs are provided in table 1.

From figure 6, we conclude that by choosing a smaller initial value of χ/f with the same initial value of m_Q, the transition of Q to zero occurs later. This behavior impacts the value of tensor perturbations T_R at the end of inflation, leading to a larger T_R if the transition happens later. Consequently, the resulting magnetic field value at the present epoch will also be larger, as demonstrated in figure 4.

B Gravitational waves and magnetic fields for higher gauge field couplings

The amplitude of GWs, computed in section 4.1, is approximately equal to their vacuum contribution. This happens because gauge field amplification is not sufficient to source metric tensor perturbations. However, for larger values of m_Q, the amplification becomes higher, leading to a sourced contribution of GWs that exceeds the vacuum value. In figure 7 we demonstrate the amplification of gravitational waves for higher values of m_Q. In this figure, we compare the results of run C1 from figure 4 (black dotted curves, with $m_Q = 2.37$) to run G (dashed red curves, with $m_Q = 5.71$) and run H (solid blue curves, with $m_Q = 2.34$) from table 1. The top left panel shows the magnetic field strength and the top right the corresponding amplification of gravitational waves. The background evolution of Q and χ/f is illustrated in the bottom left and right panels, respectively. For higher values of m_Q the backreaction effects become important earlier, forcing the system into the new backreaction-supported attractor very close to the start of our simulation. This leads to the amplification of tensor perturbations on larger scales, with the resulting peak of magnetic energy spectra at a length scale of order 10 Mpc. This shifts the peak of GWs signal towards smaller frequencies. We avoid taking higher values of m_Q, keeping in mind the constraints from bounds on perturbativity. We note that this scenario with $m_Q = 5.71$ is already well within the backreaction regime and may conflict with perturbativity bounds. Here, we aim to demonstrate how the amplification of GWs might still be achieved. However, a thorough study of such scenarios would require lattice simulations of the axion-SU(2) system.

JCAP12(2024)057

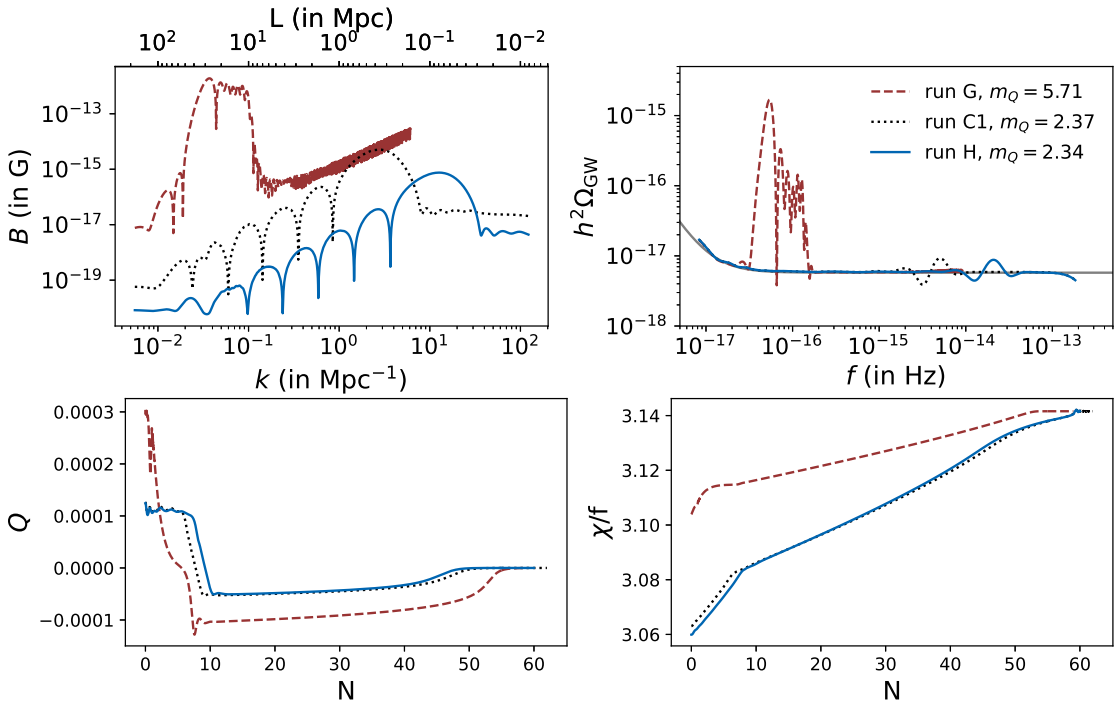

Figure 7. In this figure, we show the obtained magnetic field strength at the present epoch and the GW density fraction $\Omega_{\rm GW}h^2$ in the top panels for the run G (dashed red curves), run C1 (black dotted curves) and run H (solid blue curves). The value of m_Q is 5.71 for run G, 2.37 for run C1 and for 2.34 run H. Bottom panels show the background evolution of Q and χ/f.

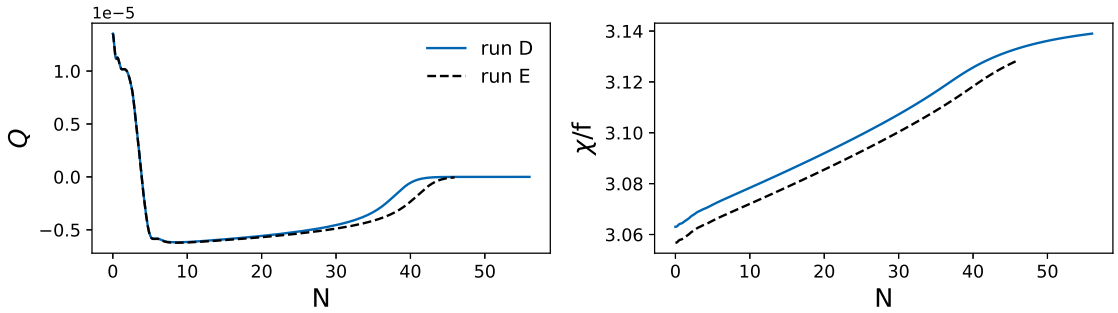

Figure 8. In this figure, we show the evolution of the Q and χ/f for the run D (solid blue curves), and E (dotted black curves). These runs are for the case $g = 0.65$.

It is worth noting that larger values of m_Q can be also achieved by choosing larger gauge field couplings. For bigger couplings, the dynamics is similar to the case with $g = 0.1$ considered in the paper, meaning that our computation is still valid for the case $g = 0.65$. The difference is that for $g = 0.65$ the backreaction of tensor perturbations on the background evolution is significant right from the beginning of inflation, even for the smallest allowed value of m_Q. Figure 8 shows two runs with $g = 0.65$ and different initial values of $\chi/f = 0.975\pi$ (run D) and 0.973π (run E), with the value of μ chosen such that the initial value of m_Q stays the same. As demonstrated in figure 8, the dynamics is similar to the evolution in figures 1 and 7, but Q transits to the backreaction-supported attractor solution at the very early stages of inflation.

JCAP12(2024)057

References

[1] L.M. Widrow, *Origin of galactic and extragalactic magnetic fields*, *Rev. Mod. Phys.* **74** (2002) 775 [astro-ph/0207240] [INSPIRE].

[2] M.L. Bernet et al., *Strong magnetic fields in normal galaxies at high redshifts*, *Nature* **454** (2008) 302 [arXiv:0807.3347] [INSPIRE].

[3] R. Beck, *Galactic and Extragalactic Magnetic Fields*, *AIP Conf. Proc.* **1085** (2009) 83 [arXiv:0810.2923] [INSPIRE].

[4] P.P. Kronberg et al., *A Global Probe of Cosmic Magnetic Fields to High Redshifts*, *Astrophys. J.* **676** (2008) 7079 [arXiv:0712.0435] [INSPIRE].

[5] T.E. Clarke, P.P. Kronberg and H. Boehringer, *A New radio-X-ray probe of galaxy cluster magnetic fields*, *Astrophys. J. Lett.* **547** (2001) L111 [astro-ph/0011281] [INSPIRE].

[6] F. Govoni and L. Feretti, *Magnetic field in clusters of galaxies*, *Int. J. Mod. Phys. D* **13** (2004) 1549 [astro-ph/0410182] [INSPIRE].

[7] C. Vogt and T.A. Ensslin, *A Bayesian view on Faraday rotation maps — Seeing the magnetic power spectra in galaxy clusters*, *Astron. Astrophys.* **434** (2005) 67 [astro-ph/0501211] [INSPIRE].

[8] A. Neronov and I. Vovk, *Evidence for strong extragalactic magnetic fields from Fermi observations of TeV blazars*, *Science* **328** (2010) 73 [arXiv:1006.3504] [INSPIRE].

[9] F. Tavecchio et al., *The intergalactic magnetic field constrained by Fermi/LAT observations of the TeV blazar 1ES 0229+200*, *Mon. Not. Roy. Astron. Soc.* **406** (2010) L70 [arXiv:1004.1329] [INSPIRE].

[10] K. Dolag, M. Kachelriess, S. Ostapchenko and R. Tomas, *Lower limit on the strength and filling factor of extragalactic magnetic fields*, *Astrophys. J. Lett.* **727** (2011) L4 [arXiv:1009.1782] [INSPIRE].

[11] W. Essey, S. Ando and A. Kusenko, *Determination of intergalactic magnetic fields from gamma ray data*, *Astropart. Phys.* **35** (2011) 135 [arXiv:1012.5313] [INSPIRE].

[12] A.M. Taylor, I. Vovk and A. Neronov, *Extragalactic magnetic fields constraints from simultaneous GeV-TeV observations of blazars*, *Astron. Astrophys.* **529** (2011) A144 [arXiv:1101.0932] [INSPIRE].

[13] K. Takahashi et al., *Lower Bounds on Magnetic Fields in Intergalactic Voids from Long-term GeV-TeV Light Curves of the Blazar Mrk 421*, *Astrophys. J. Lett.* **771** (2013) L42 [arXiv:1303.3069] [INSPIRE].

[14] FERMI-LAT collaboration, *Constraints on the Intergalactic Magnetic Field from Gamma-Ray Observations of Blazars*, *eConf C* **121028** (2012) 365 [arXiv:1303.5093] [INSPIRE].

[15] J.D. Finke et al., *Constraints on the Intergalactic Magnetic Field with Gamma-Ray Observations of Blazars*, *Astrophys. J.* **814** (2015) 20 [arXiv:1510.02485] [INSPIRE].

[16] A. Kandus, K.E. Kunze and C.G. Tsagas, *Primordial magnetogenesis*, *Phys. Rept.* **505** (2011) 1 [arXiv:1007.3891] [INSPIRE].

[17] L.M. Widrow et al., *The First Magnetic Fields*, *Space Sci. Rev.* **166** (2012) 37 [arXiv:1109.4052] [INSPIRE].

[18] R. Durrer and A. Neronov, *Cosmological Magnetic Fields: Their Generation, Evolution and Observation*, *Astron. Astrophys. Rev.* **21** (2013) 62 [arXiv:1303.7121] [INSPIRE].

JCAP12(2024)057

[19] K. Subramanian, *The origin, evolution and signatures of primordial magnetic fields*, *Rept. Prog. Phys.* **79** (2016) 076901 [arXiv:1504.02311] [INSPIRE].

[20] T. Vachaspati, *Progress on cosmological magnetic fields*, *Rept. Prog. Phys.* **84** (2021) 074901 [arXiv:2010.10525] [INSPIRE].

[21] M.S. Turner and L.M. Widrow, *Inflation Produced, Large Scale Magnetic Fields*, *Phys. Rev. D* **37** (1988) 2743 [INSPIRE].

[22] B. Ratra, *Cosmological 'seed' magnetic field from inflation*, *Astrophys. J. Lett.* **391** (1992) L1 [INSPIRE].

[23] S.M. Carroll and G.B. Field, *The Einstein equivalence principle and the polarization of radio galaxies*, *Phys. Rev. D* **43** (1991) 3789 [INSPIRE].

[24] A. Diaz-Gil, J. Garcia-Bellido, M. Garcia Perez and A. Gonzalez-Arroyo, *Magnetic field production during preheating at the electroweak scale*, *Phys. Rev. Lett.* **100** (2008) 241301 [arXiv:0712.4263] [INSPIRE].

[25] J. Martin and J. Yokoyama, *Generation of Large-Scale Magnetic Fields in Single-Field Inflation*, *JCAP* **01** (2008) 025 [arXiv:0711.4307] [INSPIRE].

[26] V. Demozzi, V. Mukhanov and H. Rubinstein, *Magnetic fields from inflation?*, *JCAP* **08** (2009) 025 [arXiv:0907.1030] [INSPIRE].

[27] S. Kanno, J. Soda and M.-A. Watanabe, *Cosmological Magnetic Fields from Inflation and Backreaction*, *JCAP* **12** (2009) 009 [arXiv:0908.3509] [INSPIRE].

[28] K. Bamba and M. Sasaki, *Large-scale magnetic fields in the inflationary universe*, *JCAP* **02** (2007) 030 [astro-ph/0611701] [INSPIRE].

[29] K.-W. Ng, S.-L. Cheng and W. Lee, *Inflationary dilaton-axion magnetogenesis*, *Chin. J. Phys.* **53** (2015) 110105 [arXiv:1409.2656] [INSPIRE].

[30] R.J.Z. Ferreira, R.K. Jain and M.S. Sloth, *Inflationary magnetogenesis without the strong coupling problem*, *JCAP* **10** (2013) 004 [arXiv:1305.7151] [INSPIRE].

[31] R.J.Z. Ferreira, R.K. Jain and M.S. Sloth, *Inflationary Magnetogenesis without the Strong Coupling Problem II: Constraints from CMB anisotropies and B-modes*, *JCAP* **06** (2014) 053 [arXiv:1403.5516] [INSPIRE].

[32] L. Campanelli, *Origin of Cosmic Magnetic Fields*, *Phys. Rev. Lett.* **111** (2013) 061301 [arXiv:1304.6534] [INSPIRE].

[33] P. Adshead, J.T. Giblin, T.R. Scully and E.I. Sfakianakis, *Magnetogenesis from axion inflation*, *JCAP* **10** (2016) 039 [arXiv:1606.08474] [INSPIRE].

[34] R. Sharma, S. Jagannathan, T.R. Seshadri and K. Subramanian, *Challenges in Inflationary Magnetogenesis: Constraints from Strong Coupling, Backreaction and the Schwinger Effect*, *Phys. Rev. D* **96** (2017) 083511 [arXiv:1708.08119] [INSPIRE].

[35] T. Fujita and R. Durrer, *Scale-invariant Helical Magnetic Fields from Inflation*, *JCAP* **09** (2019) 008 [arXiv:1904.11428] [INSPIRE].

[36] E.V. Gorbar, K. Schmitz, O.O. Sobol and S.I. Vilchinskii, *Hypermagnetogenesis from axion inflation: Model-independent estimates*, *Phys. Rev. D* **105** (2022) 043530 [arXiv:2111.04712] [INSPIRE].

[37] A. Kushwaha and S. Shankaranarayanan, *Helical magnetic fields from Riemann coupling*, *Phys. Rev. D* **102** (2020) 103528 [arXiv:2008.10825] [INSPIRE].

JCAP12(2024)057

[38] D. Maity, S. Pal and T. Paul, *Effective Theory of Inflationary Magnetogenesis and Constraints on Reheating*, *JCAP* **05** (2021) 045 [arXiv:2103.02411] [INSPIRE].

[39] S. Tripathy, D. Chowdhury, R.K. Jain and L. Sriramkumar, *Challenges in the choice of the nonconformal coupling function in inflationary magnetogenesis*, *Phys. Rev. D* **105** (2022) 063519 [arXiv:2111.01478] [INSPIRE].

[40] T. Vachaspati, *Magnetic fields from cosmological phase transitions*, *Phys. Lett. B* **265** (1991) 258 [INSPIRE].

[41] G. Sigl, A.V. Olinto and K. Jedamzik, *Primordial magnetic fields from cosmological first order phase transitions*, *Phys. Rev. D* **55** (1997) 4582 [astro-ph/9610201] [INSPIRE].

[42] A.D. Dolgov and D. Grasso, *Generation of cosmic magnetic fields and gravitational waves at neutrino decoupling*, *Phys. Rev. Lett.* **88** (2002) 011301 [astro-ph/0106154] [INSPIRE].

[43] T. Stevens et al., *Role of Charged Gauge Fields in Generating Magnetic Seed Fields in Bubble Collisions during the Cosmological Electroweak Phase Transition*, *Phys. Rev. D* **77** (2008) 023501 [arXiv:0707.1346] [INSPIRE].

[44] T. Kahniashvili, A.G. Tevzadze and B. Ratra, *Phase Transition Generated Cosmological Magnetic Field at Large Scales*, *Astrophys. J.* **726** (2011) 78 [arXiv:0907.0197] [INSPIRE].

[45] E.M. Henley, M.B. Johnson and L.S. Kisslinger, *EWPT Nucleation With MSSM and Electromagnetic Field Creation*, *Phys. Rev. D* **81** (2010) 085035 [arXiv:1001.2783] [INSPIRE].

[46] D. Grasso and H.R. Rubinstein, *Magnetic fields in the early universe*, *Phys. Rept.* **348** (2001) 163 [astro-ph/0009061] [INSPIRE].

[47] B.-L. Cheng and A.V. Olinto, *Primordial magnetic fields generated in the quark-hadron transition*, *Phys. Rev. D* **50** (1994) 2421 [INSPIRE].

[48] S. Balaji, M. Fairbairn and M.O. Olea-Romacho, *Magnetogenesis with gravitational waves and primordial black hole dark matter*, *Phys. Rev. D* **109** (2024) 075048 [arXiv:2402.05179] [INSPIRE].

[49] N. Barnaby, R. Namba and M. Peloso, *Observable non-gaussianity from gauge field production in slow roll inflation, and a challenging connection with magnetogenesis*, *Phys. Rev. D* **85** (2012) 123523 [arXiv:1202.1469] [INSPIRE].

[50] L. Campanelli, *Helical Magnetic Fields from Inflation*, *Int. J. Mod. Phys. D* **18** (2009) 1395 [arXiv:0805.0575] [INSPIRE].

[51] L. Campanelli, *Evolution of Magnetic Fields in Freely Decaying Magnetohydrodynamic Turbulence*, *Phys. Rev. Lett.* **98** (2007) 251302 [arXiv:0705.2308] [INSPIRE].

[52] R. Banerjee and K. Jedamzik, *The evolution of cosmic magnetic fields: From the very early universe, to recombination, to the present*, *Phys. Rev. D* **70** (2004) 123003 [astro-ph/0410032] [INSPIRE].

[53] D.T. Son, *Magnetohydrodynamics of the early universe and the evolution of primordial magnetic fields*, *Phys. Rev. D* **59** (1999) 063008 [hep-ph/9803412] [INSPIRE].

[54] W.D. Garretson, G.B. Field and S.M. Carroll, *Primordial magnetic fields from pseudoGoldstone bosons*, *Phys. Rev. D* **46** (1992) 5346 [hep-ph/9209238] [INSPIRE].

[55] R.Z. Ferreira and M.S. Sloth, *Universal Constraints on Axions from Inflation*, *JHEP* **12** (2014) 139 [arXiv:1409.5799] [INSPIRE].

[56] T. Prokopec, *Cosmological magnetic fields from photon coupling to fermions and bosons in inflation*, astro-ph/0106247 [INSPIRE].

JCAP12(2024)057

[57] M.M. Anber and L. Sorbo, *Naturally inflating on steep potentials through electromagnetic dissipation*, *Phys. Rev. D* **81** (2010) 043534 [arXiv:0908.4089] [INSPIRE].

[58] N. Barnaby, R. Namba and M. Peloso, *Phenomenology of a Pseudo-Scalar Inflaton: Naturally Large Nongaussianity*, *JCAP* **04** (2011) 009 [arXiv:1102.4333] [INSPIRE].

[59] N. Barnaby, E. Pajer and M. Peloso, *Gauge Field Production in Axion Inflation: Consequences for Monodromy, non-Gaussianity in the CMB, and Gravitational Waves at Interferometers*, *Phys. Rev. D* **85** (2012) 023525 [arXiv:1110.3327] [INSPIRE].

[60] M. Shiraishi, A. Ricciardone and S. Saga, *Parity violation in the CMB bispectrum by a rolling pseudoscalar*, *JCAP* **11** (2013) 051 [arXiv:1308.6769] [INSPIRE].

[61] J.L. Cook and L. Sorbo, *An inflationary model with small scalar and large tensor nongaussianities*, *JCAP* **11** (2013) 047 [arXiv:1307.7077] [INSPIRE].

[62] R.Z. Ferreira, J. Ganc, J. Noreña and M.S. Sloth, *On the validity of the perturbative description of axions during inflation*, *JCAP* **04** (2016) 039 [*Erratum ibid.* **10** (2016) E01] [arXiv:1512.06116] [INSPIRE].

[63] M. Peloso, L. Sorbo and C. Unal, *Rolling axions during inflation: perturbativity and signatures*, *JCAP* **09** (2016) 001 [arXiv:1606.00459] [INSPIRE].

[64] R. Durrer et al., *Scalar perturbations from inflation in the presence of gauge fields*, *Phys. Rev. D* **110** (2024) 043533 [arXiv:2404.19694] [INSPIRE].

[65] S.-L. Cheng, W. Lee and K.-W. Ng, *Numerical study of pseudoscalar inflation with an axion-gauge field coupling*, *Phys. Rev. D* **93** (2016) 063510 [arXiv:1508.00251] [INSPIRE].

[66] A. Notari and K. Tywoniuk, *Dissipative Axial Inflation*, *JCAP* **12** (2016) 038 [arXiv:1608.06223] [INSPIRE].

[67] O.O. Sobol, E.V. Gorbar and S.I. Vilchinskii, *Backreaction of electromagnetic fields and the Schwinger effect in pseudoscalar inflation magnetogenesis*, *Phys. Rev. D* **100** (2019) 063523 [arXiv:1907.10443] [INSPIRE].

[68] G. Dall'Agata, S. González-Martín, A. Papageorgiou and M. Peloso, *Warm dark energy*, *JCAP* **08** (2020) 032 [arXiv:1912.09950] [INSPIRE].

[69] V. Domcke, V. Guidetti, Y. Welling and A. Westphal, *Resonant backreaction in axion inflation*, *JCAP* **09** (2020) 009 [arXiv:2002.02952] [INSPIRE].

[70] M. Peloso and L. Sorbo, *Instability in axion inflation with strong backreaction from gauge modes*, *JCAP* **01** (2023) 038 [arXiv:2209.08131] [INSPIRE].

[71] A. Caravano, E. Komatsu, K.D. Lozanov and J. Weller, *Lattice simulations of axion-$U(1)$ inflation*, *Phys. Rev. D* **108** (2023) 043504 [arXiv:2204.12874] [INSPIRE].

[72] J. Garcia-Bellido, A. Papageorgiou, M. Peloso and L. Sorbo, *A flashing beacon in axion inflation: recurring bursts of gravitational waves in the strong backreaction regime*, *JCAP* **01** (2024) 034 [arXiv:2303.13425] [INSPIRE].

[73] R. von Eckardstein et al., *Axion inflation in the strong-backreaction regime: decay of the Anber-Sorbo solution*, *JHEP* **11** (2023) 183 [arXiv:2309.04254] [INSPIRE].

[74] D.G. Figueroa, J. Lizarraga, A. Urio and J. Urrestilla, *Strong Backreaction Regime in Axion Inflation*, *Phys. Rev. Lett.* **131** (2023) 151003 [arXiv:2303.17436] [INSPIRE].

[75] R. Sharma, A. Brandenburg, K. Subramanian and A. Vikman, *Lattice simulations of axion-$U(1)$ inflation: gravitational waves, magnetic fields, and black holes*, arXiv:2411.04854 [INSPIRE].

JCAP12(2024)057

[76] N. Barnaby and M. Peloso, *Large Nongaussianity in Axion Inflation*, *Phys. Rev. Lett.* **106** (2011) 181301 [arXiv:1011.1500] [INSPIRE].

[77] A. Caravano and M. Peloso, *Unveiling the nonlinear dynamics of a rolling axion during inflation*, arXiv:2407.13405 [INSPIRE].

[78] A. Linde, S. Mooij and E. Pajer, *Gauge field production in supergravity inflation: Local non-Gaussianity and primordial black holes*, *Phys. Rev. D* **87** (2013) 103506 [arXiv:1212.1693] [INSPIRE].

[79] E. Bugaev and P. Klimai, *Axion inflation with gauge field production and primordial black holes*, *Phys. Rev. D* **90** (2014) 103501 [arXiv:1312.7435] [INSPIRE].

[80] K. Freese, J.A. Frieman and A.V. Olinto, *Natural inflation with pseudo-Nambu-Goldstone bosons*, *Phys. Rev. Lett.* **65** (1990) 3233 [INSPIRE].

[81] A. Maleknejad and M.M. Sheikh-Jabbari, *Gauge-flation: Inflation From Non-Abelian Gauge Fields*, *Phys. Lett. B* **723** (2013) 224 [arXiv:1102.1513] [INSPIRE].

[82] A. Maleknejad and M.M. Sheikh-Jabbari, *Non-Abelian Gauge Field Inflation*, *Phys. Rev. D* **84** (2011) 043515 [arXiv:1102.1932] [INSPIRE].

[83] P. Adshead, E. Martinec and M. Wyman, *Perturbations in Chromo-Natural Inflation*, *JHEP* **09** (2013) 087 [arXiv:1305.2930] [INSPIRE].

[84] P. Adshead, E. Martinec and M. Wyman, *Gauge fields and inflation: Chiral gravitational waves, fluctuations, and the Lyth bound*, *Phys. Rev. D* **88** (2013) 021302 [arXiv:1301.2598] [INSPIRE].

[85] P. Adshead and M. Wyman, *Chromo-Natural Inflation: Natural inflation on a steep potential with classical non-Abelian gauge fields*, *Phys. Rev. Lett.* **108** (2012) 261302 [arXiv:1202.2366] [INSPIRE].

[86] A. Maleknejad, *Axion Inflation with an $SU(2)$ Gauge Field: Detectable Chiral Gravity Waves*, *JHEP* **07** (2016) 104 [arXiv:1604.03327] [INSPIRE].

[87] A. Papageorgiou, M. Peloso and C. Unal, *Nonlinear perturbations from the coupling of the inflaton to a non-Abelian gauge field, with a focus on Chromo-Natural Inflation*, *JCAP* **09** (2018) 030 [arXiv:1806.08313] [INSPIRE].

[88] P. Adshead, E. Martinec, E.I. Sfakianakis and M. Wyman, *Higgsed Chromo-Natural Inflation*, *JHEP* **12** (2016) 137 [arXiv:1609.04025] [INSPIRE].

[89] D.H. Lyth, *What would we learn by detecting a gravitational wave signal in the cosmic microwave background anisotropy?*, *Phys. Rev. Lett.* **78** (1997) 1861 [hep-ph/9606387] [INSPIRE].

[90] R.R. Caldwell and C. Devulder, *Axion Gauge Field Inflation and Gravitational Leptogenesis: A Lower Bound on B Modes from the Matter-Antimatter Asymmetry of the Universe*, *Phys. Rev. D* **97** (2018) 023532 [arXiv:1706.03765] [INSPIRE].

[91] I. Obata, T. Miura and J. Soda, *Chromo-Natural Inflation in the Axiverse*, *Phys. Rev. D* **92** (2015) 063516 [*Addendum ibid.* **95** (2017) 109902] [arXiv:1412.7620] [INSPIRE].

[92] I. Obata and J. Soda, *Chiral primordial Chiral primordial gravitational waves from dilaton induced delayed chromonatural inflation*, *Phys. Rev. D* **93** (2016) 123502 [*Addendum ibid.* **95** (2017) 109903] [arXiv:1602.06024] [INSPIRE].

[93] V. Domcke, B. Mares, F. Muia and M. Pieroni, *Emerging chromo-natural inflation*, *JCAP* **04** (2019) 034 [arXiv:1807.03358] [INSPIRE].

JCAP12(2024)057

[94] E. Dimastrogiovanni, M. Fasiello, M. Michelotti and L. Pinol, *Primordial gravitational waves in non-minimally coupled chromo-natural inflation*, *JCAP* **02** (2024) 039 [arXiv:2303.10718] [INSPIRE].

[95] T. Murata and T. Kobayashi, *Chromo-natural inflation supported by enhanced friction from Horndeski gravity*, *JCAP* **10** (2024) 044 [arXiv:2408.01773] [INSPIRE].

[96] P. Adshead and M. Wyman, *Gauge-flation trajectories in Chromo-Natural Inflation*, *Phys. Rev. D* **86** (2012) 043530 [arXiv:1203.2264] [INSPIRE].

[97] M.M. Sheikh-Jabbari, *Gauge-flation Vs Chromo-Natural Inflation*, *Phys. Lett. B* **717** (2012) 6 [arXiv:1203.2265] [INSPIRE].

[98] A. Maleknejad and M. Zarei, *Slow-roll trajectories in Chromo-Natural and Gauge-flation Models, an exhaustive analysis*, *Phys. Rev. D* **88** (2013) 043509 [arXiv:1212.6760] [INSPIRE].

[99] A. Maleknejad, M.M. Sheikh-Jabbari and J. Soda, *Gauge Fields and Inflation*, *Phys. Rept.* **528** (2013) 161 [arXiv:1212.2921] [INSPIRE].

[100] O. Iarygina and E.I. Sfakianakis, *Gravitational waves from spectator Gauge-flation*, *JCAP* **11** (2021) 023 [arXiv:2105.06972] [INSPIRE].

[101] E. Dimastrogiovanni, M. Fasiello and T. Fujita, *Primordial Gravitational Waves from Axion-Gauge Fields Dynamics*, *JCAP* **01** (2017) 019 [arXiv:1608.04216] [INSPIRE].

[102] T. Fujita, R. Namba and Y. Tada, *Does the detection of primordial gravitational waves exclude low energy inflation?*, *Phys. Lett. B* **778** (2018) 17 [arXiv:1705.01533] [INSPIRE].

[103] T. Fujita, E.I. Sfakianakis and M. Shiraishi, *Tensor Spectra Templates for Axion-Gauge Fields Dynamics during Inflation*, *JCAP* **05** (2019) 057 [arXiv:1812.03667] [INSPIRE].

[104] O. Iarygina, E.I. Sfakianakis, R. Sharma and A. Brandenburg, *Backreaction of axion-SU(2) dynamics during inflation*, *JCAP* **04** (2024) 018 [arXiv:2311.07557] [INSPIRE].

[105] E. Dimastrogiovanni, M. Fasiello and A. Papageorgiou, *Novel primordial black hole production mechanism from non-Abelian gauge fields during inflation*, *Phys. Rev. D* **110** (2024) 103542 [arXiv:2403.13581] [INSPIRE].

[106] E. Dimastrogiovanni, M. Fasiello, M. Michelotti and O. Özsoy, *A universal constraint on axion non-Abelian dynamics during inflation*, arXiv:2405.17411 [INSPIRE].

[107] S. Alexander, C. Creque-Sarbinowski, H. Gilmer and K. Freese, *Higgs Inflation and the Electroweak Gauge Sector*, arXiv:2306.04671 [INSPIRE].

[108] A. Brandenburg et al., *Evolution of hydromagnetic turbulence from the electroweak phase transition*, *Phys. Rev. D* **96** (2017) 123528 [arXiv:1711.03804] [INSPIRE].

[109] K. Kamada, F. Uchida and J. Yokoyama, *Baryon isocurvature constraints on the primordial hypermagnetic fields*, *JCAP* **04** (2021) 034 [arXiv:2012.14435] [INSPIRE].

[110] K. Kamada and A.J. Long, *Evolution of the Baryon Asymmetry through the Electroweak Crossover in the Presence of a Helical Magnetic Field*, *Phys. Rev. D* **94** (2016) 123509 [arXiv:1610.03074] [INSPIRE].

[111] A. Maleknejad and E. Erfani, *Chromo-Natural Model in Anisotropic Background*, *JCAP* **03** (2014) 016 [arXiv:1311.3361] [INSPIRE].

[112] A. Papageorgiou, M. Peloso and C. Unal, *Nonlinear perturbations from axion-gauge fields dynamics during inflation*, *JCAP* **07** (2019) 004 [arXiv:1904.01488] [INSPIRE].

JCAP12(2024)057

[113] E. Dimastrogiovanni and M. Peloso, *Stability analysis of chromo-natural inflation and possible evasion of Lyth's bound*, *Phys. Rev. D* **87** (2013) 103501 [arXiv:1212.5184] [INSPIRE].

[114] R. Namba et al., *Scale-dependent gravitational waves from a rolling axion*, *JCAP* **01** (2016) 041 [arXiv:1509.07521] [INSPIRE].

[115] A. Maleknejad and E. Komatsu, *Production and Backreaction of Spin-2 Particles of SU(2) Gauge Field during Inflation*, *JHEP* **05** (2019) 174 [arXiv:1808.09076] [INSPIRE].

[116] K. Ishiwata, E. Komatsu and I. Obata, *Axion-gauge field dynamics with backreaction*, *JCAP* **03** (2022) 010 [arXiv:2111.14429] [INSPIRE].

[117] R. Kallosh and A. Linde, *Universality Class in Conformal Inflation*, *JCAP* **07** (2013) 002 [arXiv:1306.5220] [INSPIRE].

[118] R. Kallosh, A. Linde and D. Roest, *Superconformal Inflationary α-Attractors*, *JHEP* **11** (2013) 198 [arXiv:1311.0472] [INSPIRE].

[119] Pencil Code collaboration, *The Pencil Code, a modular MPI code for partial differential equations and particles: multipurpose and multiuser-maintained*, *J. Open Source Softw.* **6** (2021) 2807 [arXiv:2009.08231] [INSPIRE].

[120] P. Adshead, J.T. Giblin, T.R. Scully and E.I. Sfakianakis, *Gauge-preheating and the end of axion inflation*, *JCAP* **12** (2015) 034 [arXiv:1502.06506] [INSPIRE].

[121] R. Sharma, K. Subramanian and T.R. Seshadri, *Generation of helical magnetic field in a viable scenario of inflationary magnetogenesis*, *Phys. Rev. D* **97** (2018) 083503 [arXiv:1802.04847] [INSPIRE].

[122] MAGIC collaboration, *A lower bound on intergalactic magnetic fields from time variability of 1ES 0229+200 from MAGIC and Fermi/LAT observations*, *Astron. Astrophys.* **670** (2023) A145 [arXiv:2210.03321] [INSPIRE].

[123] Planck collaboration, *Planck 2015 results. XIX. Constraints on primordial magnetic fields*, *Astron. Astrophys.* **594** (2016) A19 [arXiv:1502.01594] [INSPIRE].

[124] P.P. Kronberg, *Extragalactic magnetic fields*, *Rept. Prog. Phys.* **57** (1994) 325 [INSPIRE].

[125] T. Fujita et al., *Consistent generation of magnetic fields in axion inflation models*, *JCAP* **05** (2015) 054 [arXiv:1503.05802] [INSPIRE].

[126] D.J. Gross, R.D. Pisarski and L.G. Yaffe, *QCD and Instantons at Finite Temperature*, *Rev. Mod. Phys.* **53** (1981) 43 [INSPIRE].

[127] A. Maleknejad, *Chiral anomaly in $SU(2)_R$-axion inflation and the new prediction for particle cosmology*, *JHEP* **06** (2020) 113 [arXiv:2103.14611] [INSPIRE].

[128] T. Patel and T. Vachaspati, *Annihilation of electroweak dumbbells*, *JHEP* **02** (2024) 164 [arXiv:2311.00026] [INSPIRE].

[129] O. Iarygina, E.I. Sfakianakis, R. Sharma and A. Brandenburg, *Datasets of "Magnetogenesis from axion-SU(2) inflation"*, v2024.12.13, DOI:10.5281/zenodo.14434086 [http://norlx65.nordita.org/~brandenb/projects/magnetogenesis-SU2/].

JCAP12(2024)057